CHALMERS
UNIVERSITY OF TECHNOLOGY

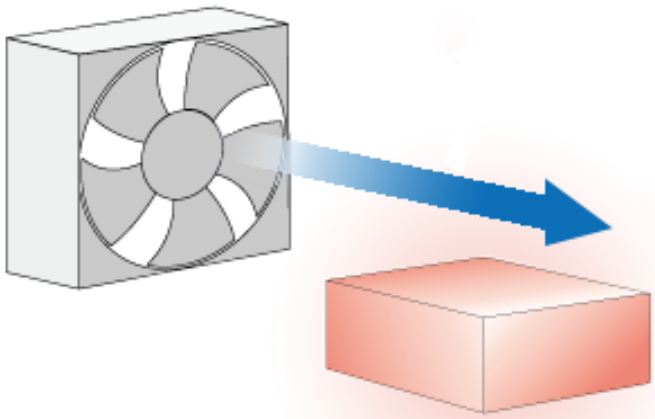

Thermal Modelling of Heat Transfer Between Ambient Air and Powerpack

A research project with Volvo Cars

Master's Thesis in Applied Mechanics

Axel Larsson

Sunil Rangaswamy

DEPARTMENT OF MECHANICS AND MARITIME SCIENCES

CHALMERS UNIVERSITY OF TECHNOLOGY
Gothenburg, Sweden 2023
www.chalmers.se

Master's thesis 2023

Thermal Modelling of Heat Transfer Between Ambient Air and Powerpack

A research project with Volvo Cars

Axel Larsson
Sunil Rangaswamy

VOLVO

CHALMERS
UNIVERSITY OF TECHNOLOGY

Department of Mechanics and Maritime Sciences
Chalmers University of Technology
Gothenburg, Sweden 2023

Thermal Modelling of Heat Transfer Between Ambient Air and Powerpack
Axel Larsson, Sunil Rangaswamy

Supervisor: Nils Basse, Volvo Cars, Sweden
Examiner: Hua-Dong Yao, Department of Mechanics and Maritime Sciences

Master's Thesis 2023
Department of Mechanics and Maritime Sciences
Chalmers University of Technology
SE-412 96 Gothenburg
Telephone +46 31 772 1000

Cover: The title page image depicts a fan forcing air over a hot surface representing the forced convection on the electric powerpack.

Typeset in LaTeX

Abstract

This report presents the creation and evaluation of an air-cooling steady state model for a Volvo Cars powerpack. It should simulate the heat transfer and temperatures from the components of the powerpack. Especially interesting is how the NVH (Noise Vibration Harshness) encapsulation affects the cooling performance. This encapsulation is a thin foam layer that surrounds the motor and dampens the noise caused by it. A 1D model already existed that handled the internal heat generation and the liquid cooling of the powerpack. Twenty chosen operating conditions were iteratively calibrated between the 1D model and a full car 3D model to yield heat transfer coefficients (HTC) for each thermal node in the extension. They were chosen as variable sweeps (sweeping over multiple values for one variable while keeping the rest constant) from a central base case, yielding four to five data points to analyse each variable's impact separately. The results show that the air-cooling increases as a fraction of the total cooling as the car velocity and driveshaft torque increases. It also shows that most air-cooling bypasses the encapsulation, meaning the encapsulation has little impact on the performance. When compared with physical measurements the accuracy of the model is low. This is most likely caused by the lack of calibration for operating conditions where multiple variables were changed from the base case. It is therefore recommended that future work includes additional operating conditions to simulate. This could not be done in this project due to time and computational constraints.

Keywords: Air cooling, BEV, GT-SUITE, Powerpack, Simulation, STAR-CCM+, Temperature, Thermal management

Acknowledgements

This thesis work is carried out between Volvo Cars and Chalmers University of Technology at Volvo Car Corporation Headquarters in Göteborg, Sweden. Thesis work is supervised by Nils Basse from Volvo Cars and Assoc. Prof. HuaDong Yao from Chalmers University of Technology.

First of all, we would like to thank Eva Haglund, Manager of electric driveline dimensioning team, for considering us to carry out this project work. We would like to thank Nils Basse for Supervising and mentoring us in each and every stage of our work. Without his guidance and support this thesis would not have been possible. We would like to show gratitude to a Assoc. Prof. HuaDong Yao, examiner from Chalmers University of Technology who provided academic support and guidance.

A warm thanks to Umut Cirik, for providing the 3D CFD model to perform full car CFD simulations. Also assisting us in every stage of 3D simulations. His support played a key role to conduct many CFD simulations.

A warm thanks to Johan Stjärnesund, for providing real car measurement data and assisting us in identifying the sensor positions and their corresponding names.

Last but not least, we would to thank all the team members of Thermo-fluids team in helping us in clarifying our doubts and supporting us when ever we needed help.

Axel Larsson, Sunil Rangaswamy, Gothenburg, June 2023

List of Acronyms

Below is the list of acronyms that have been used throughout this thesis listed in alphabetical order:

1D	One Dimensional
3D	Three Dimensional
AWD	All Wheel Drive
BEV	Battery Electric Vehicle
CAE	Computer Aided Engineering
CFD	Computation Fluid Dynamics
CVTM	Complete Vehicle Thermal Model
EFAD	Electric Front Axle Drive
E-Machine	Electric machine
EMS	Energy Management System
ERAD	Electric Rear Axle Drive
EV	Electric Vehicle
HTC	Heat Transfer Coefficient
ICE	Internal Combustion Engine
NVH	Noise Vibration Harshness
RMF	Rotating Magnetic field
TDR	Turbulent Dissipation Rate
TKE	Turbulent Kinetic Energy

Contents

List of Figures

List of Tables

1
Introduction

This chapter presents the background, aim and limitations of the master thesis project.

1.1 Background

The automotive industry in Europe is one of the dominant industries. It has been observed that almost all the major players of the automotive sector are seeking a substantial transformation in their drive trains from internal combustion engines to first hybrids and now more and more towards fully electric vehicles. Volvo is no exception in this. As per CNBC report, the number of electric cars, buses, vans and heavy trucks on roads is expected to hit 145 million by 2030, the International Energy Agency [1].

In these electric vehicles the thermal management is of great importance. In the case of over-heating, components may get damaged. Better cooling also improves the efficiency and performance of the electric powerpack. It is therefore crucial to be able to accurately model and understand what factors influence the cooling of the powerpack and what can be done to improve it.

At the Electric Drive-line department at Volvo Cars the modelling of the powerpack is handled with CAE (Computer Aided Engineering) tools. So far the powerpack cooling model that is used only takes into account liquid cooling. It would be advantageous to also have a model that can accurately and cheaply model the air cooling from the powerpack to the air inside the car. Air cooling can be very crucial at higher vehicle speeds as well as in winter seasons when air temperatures are low. A model to accurately calculate this behaviour is therefore requested.

1.2 Aim

The aim of the project is to construct a thermal model add-on in GT-SUITE that models the bi-directional heat flow between the powerpack and the air. The model should take a number of variables as input. One category of these are the internal factors of supplied voltage, torque on the driveshaft, and driveshaft rpm. These determine the internal heat generation of the powerpack. The other category are the external factors of vehicle velocity, radiator rejected heat, inlet fan speed, and ambient temperature. These affect the temperature and velocity of the air inside the car. This will be modelled for both front and rear powerpacks.

The 1D model with these variables as input should accurately be able to match real values measured for the P519 powerpack.

1.3 Limitations

A 3D model would be more accurate and would be able to catch local results for different regions of the powerpack and its encapsulation. But due to the substantial computational cost that would be required a simpler 1D model will be created to more easily receive an approximate solution for a given operating condition.

To reduce complexity the model will ignore conduction between the powerpack parts. The electric motor and the transmission are in contact with each other and conduction can occur there but it will not be modelled. That is partly because it would be complicated to determine how much heat is transferred there but also because the total heat transfer out from the powerpack is not affected by internal heat transfers.

In the 1D Thermal model both the front and rear powerpacks are analysed separately to reduce complex interactions. The models are not dependent on each other so input variables were identical for both during simulations.

Due to limitation of time and lack of readily available measurement data, results from the 1D model will be calibrated to 3D CFD model. Practical limitations in the placement of the temperature sensors made it difficult to validate the results of each case with measured data. Therefore, comparisons with measurement data are done based on availability.

Our scope of work is limited to performing steady state simulations due to the requirement of high computational time and cost that would be necessary to perform transient simulations for the full car.

Finally our aim primarily concerns the air cooling of the powerpack and its impact on the total cooling. The actual internal operation and heat generation within the powerpack will therefore only be covered in brief when necessary.

2

Theory

This Chapter provides insight information about the parts such as E-Machine, Transmission, Inverter which are collectively defined as the Powerpack. Followed by a short description on Encapsulation which encloses the powerpacks. Modes of Heat transfer and theory on thermodynamics parameters used in our thesis work are described next. Followed by a brief explanation of the existing 1D thermal model and information on the tools which are used for our work like STAR-CCM+ for 3D CFD simulations & GT-SUITE for 1D thermal modelling.

2.1 Powerpacks

Powerpack is the integral part of the modular electric powertrain that includes E-Machine, Transmission and Inverter. Based on the type of vehicle, the size of the powerpack varies. For AWD (All Wheel Drive) vehicle, two powerpack is observed one at the front to transfer power to front wheels and another powerpack for the rear wheels. One powerpack is good enough for regular day to day use either in the front axle or the rear axle. Since, EV´s are getting popular from past couple of years. Optimising the performance and its efficiency is key to success of any EV. Refined and Efficient powerpack plays a vital role for any EV.

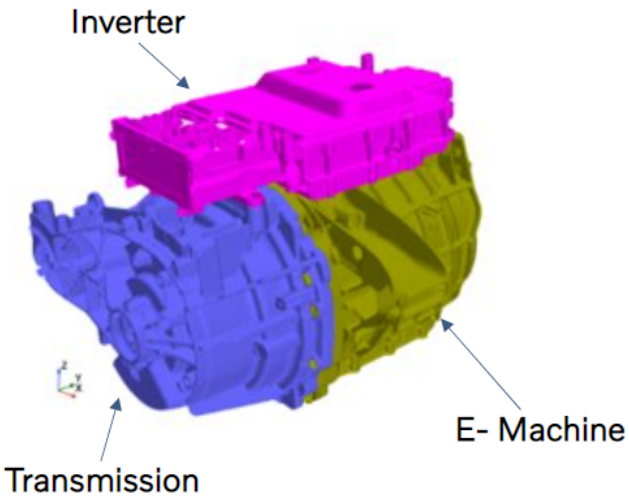

Figure 2.1: Powerpack

2.2 E-machine / Electric motor/generator

Electric motor is a core component of an electric Vehicle. In general electric motor has two major parts Rotor and a stator. The rotor, as name itself explains, is the lone rotating part which is analogous to a crankshaft which feeds torque from transmission to the differentials. Stator is the stationary outer shell, whose housing is mounted to chassis like an engine block. Electric motor can be of two types asynchronous and synchronous. The asynchronous motor is also known as induction motor, to generate rotating magnetic field (RMF) from the stator, rotor is spinned. Asynchronous motors generate high power output hence it is commonly used in electric vehicles. On the other hand in the synchronous motor, rotor rotates in the same speeds as the magnetic field. Therefore, at low speeds high torque can be achieved. This motor is suitable for urban driving. Synchronous motors in general are of less weight and compact.

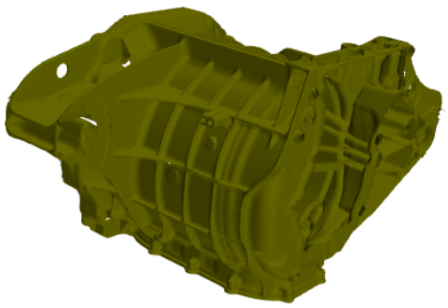

Figure 2.2: E-machine

2.3 Transmission

The main purpose of transmission in any automobile is to transfer power from the engine to driveshaft and to the differentials to spin the wheels. The transmission varies the torque, speed of the vehicle and direction by changing the ratio of the transmission which enables to have high torque once the vehicle starts. Internal combustion engine requires multi-speed transmission to achieve power output at varied operating conditions. Whereas, Electric motors in Battery electric vehicle generates consistent quantity of torque within a specific range for any given rpm. Electric motors can generate power instantly with a quick time, hence generating the torque by revving as in ICE is not necessary. EV has single transmission ratio´s.

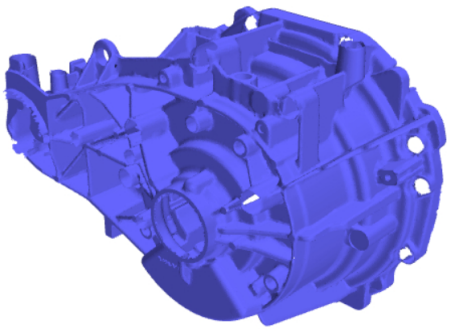

Figure 2.3: Transmission

2.4 Inverter

Inverter is an electronic device which converts DC current into AC output.It is a key component for any electric vehicle. Electric current which is stored in batteries after recharging will be in DC format. It is difficult to control the vehicle speed and torque with DC power supply. Hence to convert DC into AC Inverter is essential. For EV, it is required to operate Electric motor smoothly on variety of driving condition. Inverter controls the electric motor. Inverter works similar to Engine Management system (EMS) used in ICE vehicles which determines the driving behaviour. Apart from driving the Electric motor, inverter also captures the regenerated energy when the breaks are applied.

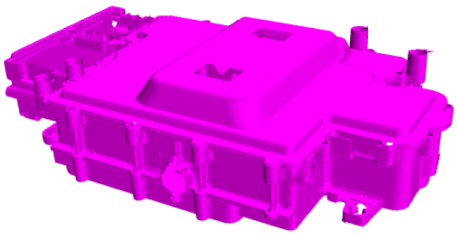

Figure 2.4: Inverter

2.5 Encapsulation

The stringent acoustic requirements are driving the need to have efficient encapsulation which covers the Power packs. Main purpose of the encapsulation is to provide good NVH i.e keep the noise as low as possible. Encapsulation are made of different materials. Size and shapes varies from one vehicle to other.

Figure 2.5: Encapsulation

2.6 Modes of Heat transfer

Basically, heat transfer takes place in 3 possible modes Conduction, Convection & Radiation. A short note about them will be follows.

2.6.1 Conduction

Conduction mode of Heat Transfer refers to transfer of heat between two parts or objects which are of different temperatures through molecular movement. The governing equation for conduction is given Fourier´s law and it states that rate of heat transfer is linearly proportional to temperature gradient [2].

$$q_k = -k\frac{dT}{dx} \tag{2.1}$$

where, q_k = Rate of heat flux in W/m^2
k = Thermal conductivity in W/m K.
dT/dx = Temperature gradient.

2.6.2 Convection

Convection is the mode of heat transfer that occurs in liquids and gasses. Transfer of heat occurs from one place to another by movement of fluids. Molecules carry heat with them when they move from one place to another place. Convection can occur in two ways, one is by free convection or natural convection which occurs due to buoyancy forces. Temperature & density difference in the fluids are major factor of buoyancy force. Whereas for the forced convection external aid such as fan or pump is essential. Convective heat transfer $\dot{Q}_c$ can be calculated using below equation which is called as Newton´s law of cooling [2].

$$\dot{Q}_c = hA\Delta T \tag{2.2}$$

where, $\dot{Q}_c$ = Rate of heat flux in W
h = heat transfer co-efficient.

A = Area in m^2.
ΔT = Temperature difference.

2.6.3 Radiation

In the case of radiation mode of Heat transfer, heat transfer from one body to another in the form of electromagnetic waves. These electromagnetic waves are mostly in the infrared region. For radiation no medium is required and to transfer energy no physical contact as well. For instance heat transfer from sun to earth takes place through vacuum.

Radiation mode of heat transfer can be calculated using Stefan -Boltzmann´s law which states that " rate of heat transfer for a black body per unit area is directly proportional to fourth power of the body temperature [2].

$$q_r = \sigma A T^4 \tag{2.3}$$

where, q_r = Radiation heat transfer in W.
σ = Stefan Boltzmann constant= 5.670×10^{-8} W/($m^2 \cdot K^4$)
A = Area in m^2.
T = Absolute temperature in K.

2.7 Relevant thermodynamic properties.

2.7.1 Thermal resistances

Thermal resistance is a heat property. It is a measurement of resistance to heat flow by a component or a material. It is nothing but the reciprocal of thermal conductance, which is the ability to conduct heat. Thermal resistance depends on the temperature difference between two points by heat flow between them. Higher thermal resistance, more difficult for heat conduction [2].

$$\text{Thermal resistance}, (R) = \frac{L}{(KA)} \tag{2.4}$$

where, L = length of the material in m.
K = Thermal conductivity in W/Km.
A = cross-sectional area in m^2.
At steady state condition, thermal capacitance will be zero.

2.7.2 Heat transfer Coefficients (HTC)

Heat transfer takes place, when there is temperature difference between two media. HTC is not a constant number it varies based on the material type, its geometry, and velocity of the fluid. HTC, calculates how much heat is transferred through the unit area of space with temperature difference of unit Kelvin.

Often, heat transfer coefficient is calculated by taking ratio of total heat flux divided by temperature difference [2].

$$\mathrm{HTC}(h) = \frac{q}{(\Delta T)} \tag{2.5}$$

where, q = Heat flux in W/m^2
ΔT = Temperature difference.

2.8 STAR-CCM+

SimCenter STAR-CCM+ software is from Siemens which is widely used to perform multi physics CFD analysis. STAR-CCM+ is a integrated software, a total package which includes everything from creation of geometry, pre-processing activities such as mesh creation with versatile meshing techniques for every needs. For example, wrapped meshing method which helps to create automated mesh with a quick time. Other meshing methods can be used if you are looking for more accurate results. In addition, complex multi-physics CFD simulation, post-processing of results can be carried out within this single software. This integration of different package makes STAR-CCM+ to standout from other commercial software‘s which provides user to come up with a effective designs solutions with less time. STAR-CCM+ can simulate both steady state and transient simulations. It works in both Windows and Linux platforms. It is one of the widely used simulation software in automotive industry. STAR-CCM+ has good help centre to resolve our issue which is very essential for smooth execution of work for live projects.[3].

Our project work involves lot of 3D CFD simulations. Above mentioned features of STAR-CCM+ made us to consider this tool for our work.

2.9 GT-SUITE

GT-SUITE is one of the leading 1D simulation tool with wide range of library such as flow library (any fluid, gas or liquid mixtures), acoustic library, Thermal library (all type of heat transfer) and many more other libraries as well. It offers users the functionalities from initial concept design phase till the detailed analysis of the components or the system we are working with. GT-SUITE has capabilities to work effectively in wide range of applications. It has distributed computing which complete the simulation faster. GT-SUITE has fusion of 3D and 1D in a same tool. It features optimisation and DOE (Design of Experiments), which provides better analysis between input parameters of the model and outputs. Our Project work involves 1D Thermal modelling and GT-SUITE performs best in this. Hence, GT-SUITE tool is employed for 1D Thermal modelling in our work [4].

2.10 Prior work

The model was not created from scratch. It is based on a prior model which in turn is based on a thermal model for a permanent magnet electric motor by Joachim Lindström [5]. This model is presented in figure 2.6. It models the internal components as thermal nodes with thermal resistances connecting them. Together they all

generate and/or transfer heat that the coolant at the top of the model must remove from the powerpack lest it melt.

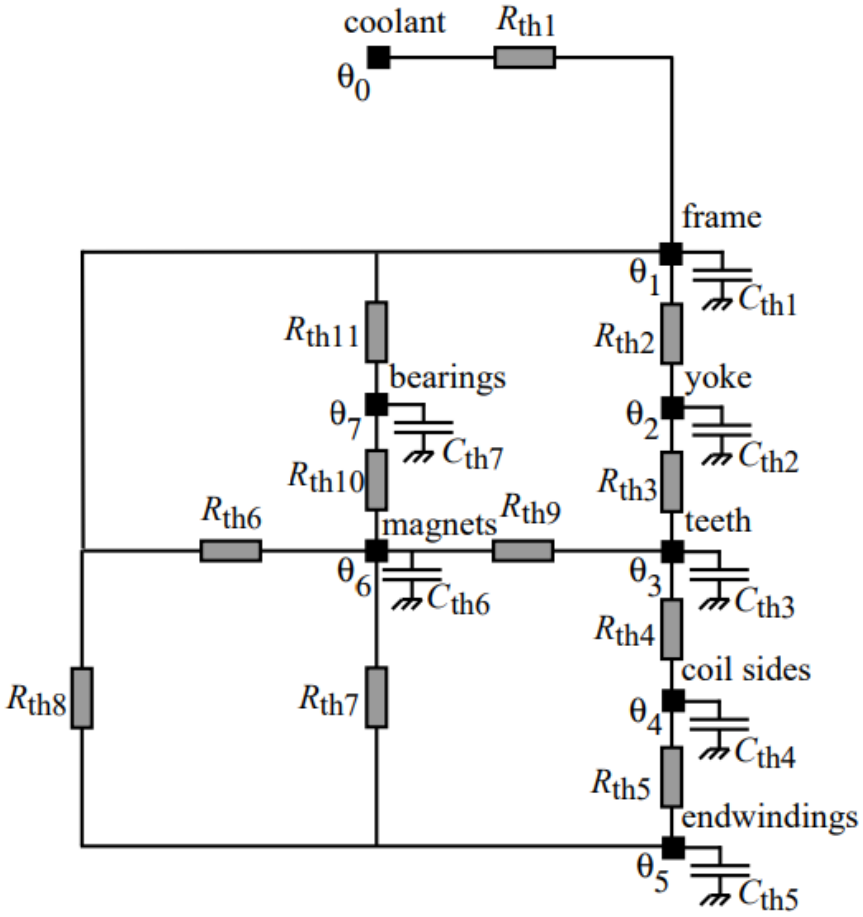

Figure 2.6: Theory E-machine thermal model

2.10.1 Existing 1D thermal model

The actual GT-Suite model provided to us by the Thermal Fluids department has clear similarities to Lindström's model. As seen in figure 2.7 it has the same internal thermal nodes for the E-machine. The major difference to the theoretical model is that an extra two thermal nodes for modelling the transmission and its lubricating oil has been added. The E-machine and transmission each have their own frame thermal node that connects to the liquid coolant.

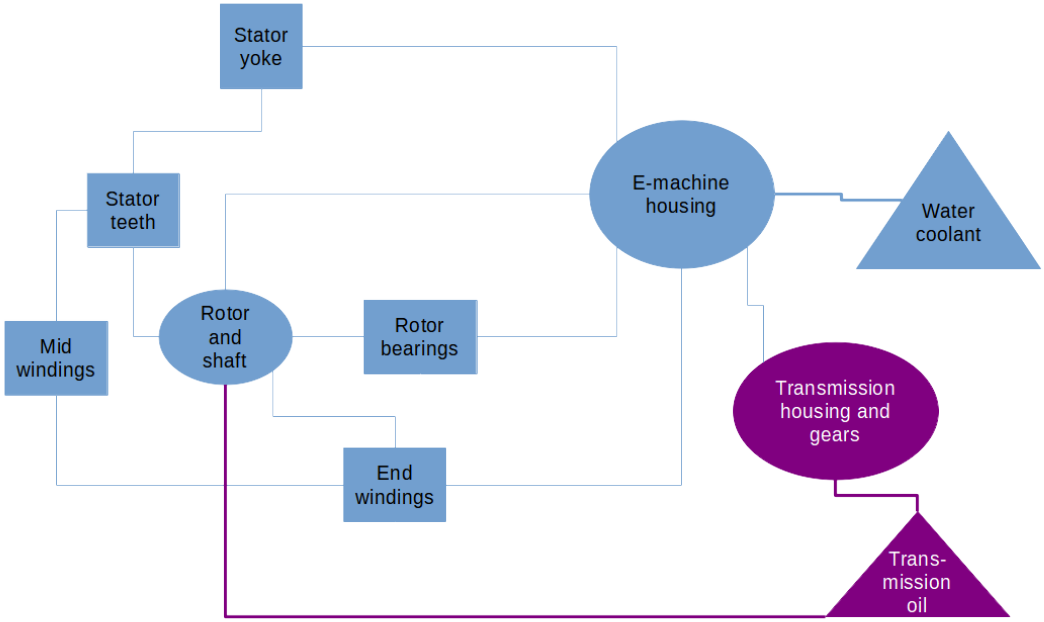

Figure 2.7: Existing 1D GT-SUITE model

3

Method

This section details the methods and procedures for how the thesis was carried out. First the two models, 1D GT-SUITE and 3D STAR-CCM+, that were used to run the simulations on are presented. Then the operating conditions selected to calibrate those models are presented followed by a section describing the iterative simulation process. Finally the procedure for acquisition of physical measurements for validation is explained.

3.1 GT-SUITE air-cooling extension

The existing model already modelled the internal resistances and the liquid cooling of the powerpack but it did not compute the air-cooling. For this an extension needed to be built. The frames of the E-machine, the transmission and the inverter from the existing model were all connected to a common thermal node with resistance connections. This common node models an average temperature for the air between the encapsulation and the powerpack. Surface areas for the resistance connection were taken from the STAR-CCM+ model while the resistance were calibrated through simulations.

From the common "inside encapsulation" node the heat flow path diverges in two, one path connects to the encapsulation inner surface with a resistance connection and the other connects directly to the engine bay ambient air through a convection connection. This modelling decision was taken because the encapsulation does not cover the entire powerpack and a portion of the heat transfer will bypass it entirely and release heat directly into the engine bay ambient air. The first part then connects to the outer surface of the encapsulation through another resistance connection and finally connects from there to the engine bay ambient air through a convection connection. Just as before the surface areas for the connections were taken from STAR-CCM+ and the resistances and HTCs respectively were found through calibration.

This final node representing the air temperature of the engine bay is a fixed temperature node. The temperature was also calibrated as a function of the input variables. This temperature and the HTCs and resistances to the connections are controlled through look-up tables that gives the values as a function of the input variables. A picture of this GT-suite extension is presented in figure 3.1.

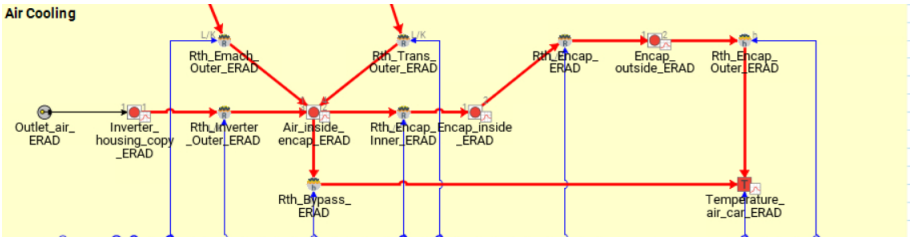

Figure 3.1: The air-cooling extension of the GT-Suite model. On the far left the imported connection from the inverter model duplicates and models the inverter frame. The two lines from the top also connects the E-machine and transmission frames to the "air inside encapsulation" node. From there the upper line models the heat transfer through the encapsulation while the lower one models the heat bypassing it. On the lower right corner a fixed temperature node sets the engine bay temperature.

3.2 Star-ccm+ 3D model

3D CFD simulations in our project is carried out using STAR-CCM+, a commercial simulation software. Simulation is carried out for Complete Vehicle Thermal model (CVTM) with a mesh count of 18.5 million cells. Our Simulation are simulated at fixed shutter position which is fully opened. It is required to generate separate meshes for every different shutter positions. To generate mesh for the whole car in a quick time, wrapping method which is one of the unique feature in STAR CCM+ is considered which generates good quality meshes. Figure 3.2 shows meshes created for powerpack components. Figure 3.3 & 3.4 shows the cut section of the meshes in different planes, which shows well refined meshes with smaller cells sizes in the critical regions and optimal mesh size in the other region.

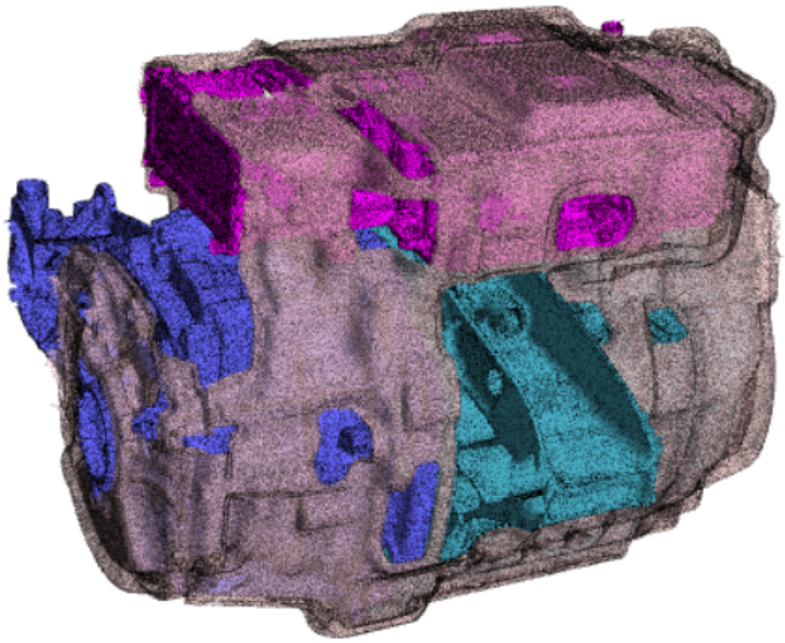

Figure 3.2: Mesh on the powerpack

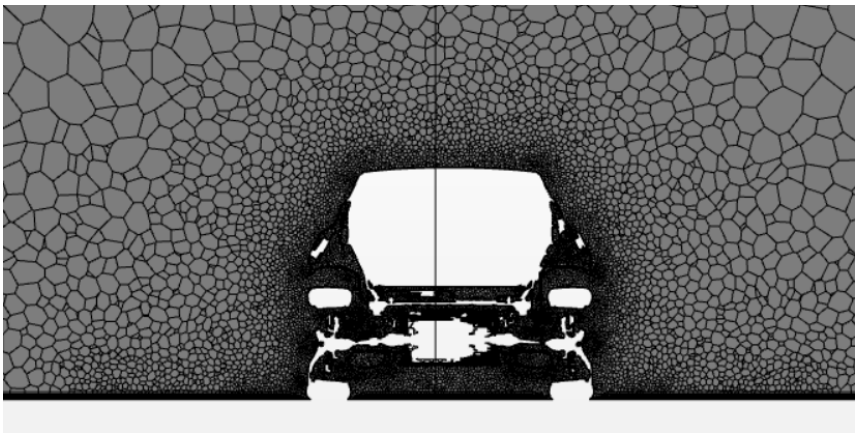

Figure 3.3: Overall Mesh Front view

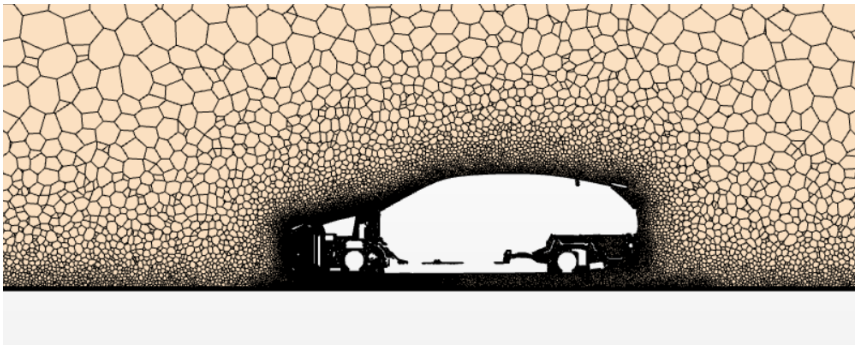

Figure 3.4: Overall Mesh side view

To accurately estimate the temperature in the air which is immediately outside the powerpacks between the powerpacks and encapsulation and also heat transfer through this encapsulation and its effect on the overall cooling of the powerpack. The gap between the powerpack and encapsulation is very small. Hence, to capture thermal property in the region well refined mesh is created for both EFAD and ERAD.

In our work full car 3D Simulations, simulated a set of 20 cases with different variable sweep which will be explained in the later stage of the report. It is a iterative process between 3D simulations and 1D simulations. On an average 2 to 3 iteration are performed between for each variable sweep. Hence, altogether more than 50 3D simulations are simulated. Hence, only Steady state simulation are carried out due to higher computational time and cost involved with Transient simulations.

Input conditions to perform CFD simulations are listed below.

- Ambient temperature in K which is outside the car
- Speed of the vehicle in Km/hr
- Temperature in K for E-machine, Inverter & Transmission (Input from 1D GT Model(Input from 1D GT Model [refer section 3.4])
- Fan Speed in rpm
- Target heat rejection in KW

In ID Thermal model, there is one thermal node which account for temperature outside the powerpack. It is iterative process between 1D simulation and 3D CFD simulation. Hence, temperature values outside the powerpacks are of prime importance. Air temperature outside the powerpacks varies at different location. For example zone near to inverter has low temperature compared to E-machine and transmission. It is extremely import to arrive at one temperature which takes the average of them. To extract average temperature probes are created which surrounds the powerpacks for both EFAD and ERAD as shown in the figure. Also, in our 1D model we have one thermal node outside the encapsulation.

To extract average temperature probes are created outside the encapsulation surrounding to it. Figure 3.5 shows the probes position for EFAD and ERAD. The probes inside the encapsulation is highlighted in red colour and yellow colour for outside the encapsulation respectively for EFAD and ERAD.

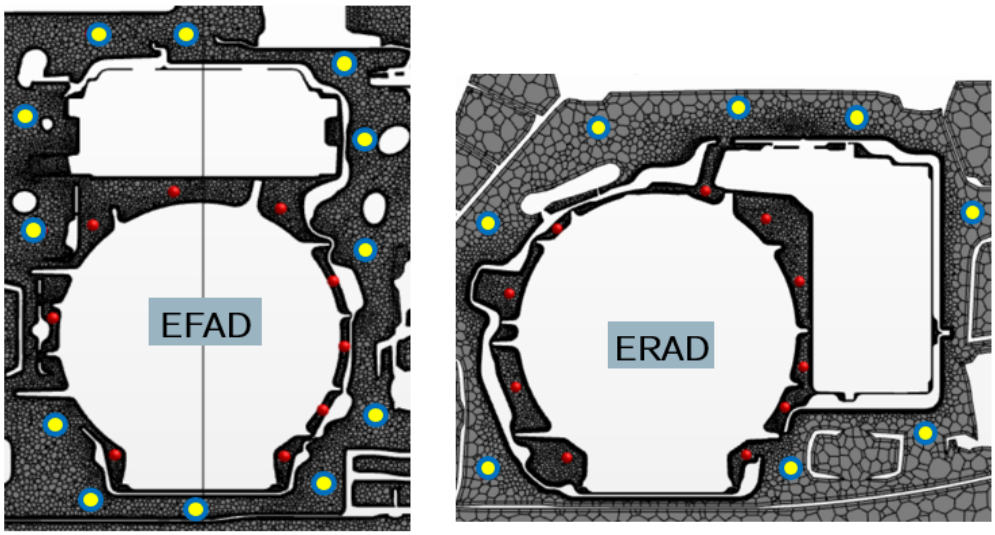

Figure 3.5: Probes in EFAD and ERAD Regions

To have a converged solution, maximum number of iteration is set to 10000. Simulation are done using High Performance Cluster (HPC) at Volvo Cars & 960 cores are used for each simulations. In general, on an average each simulation took 8 hours to attain convergence. To monitor the proper convergence residual monitors of continuity, energy, TDR (turbulent dissipation rate), TKE (turbulent kinetic energy), and X, y, Z-momentum are monitored.

Temperature and Heat Transfer values are extracted for both EFAD and ERAD by creating reports individually for each component of the powerpacks.

3.3 Operating conditions

To properly calibrate the model a number of fixed operating conditions were simulated. First a base case was chosen from which all other cases were derived. The operating condition for the base case is shown in table 3.1. All other cases were identical to the base case except for the change in a single variable each. This was done so that the effect for each variable could be isolated and analysed separately.

Table 3.1: Operating condition for the base case.

Velocity	100 km/h
Torque	200 Nm
Voltage	200 V
Ambient temperature	15 ° C
Fan speed	3200 rpm
Radiator rejected heat	10 kW

The individual cases that were simulated are presented in table 3.2. These were chosen to cover a representative range of the variables that could exist during normal

driving conditions. This adds up 19 total cases that were simulated and four data point for each variable to analyse and calibrate the GT-Suite model on. For all cases the liquid coolant temperature was a constant 293 K. In reality the coolant temperature should be dependent on the heat rejection through the radiator but for ease of modelling they were treated as independent factors.

Table 3.2: Variable sweep cases for the six chosen input variables. Do note that the base case presented above added another data point to all the variable sweeps. The variable for the velocity sweep had one more data case than the other variable sweeps.

Velocity [km/h]	10	30	50	180
Torque [Nm]	0	100	400	N/A
Voltage [V]	300	400	450	N/A
Ambient temperature [° C]	-10	0	35	N/A
Fan speed [rpm]	0	800	1600	N/A
Radiator rejected heat [kW]	0	5	20	N/A

It should be noted here that the preexisting GT-SUITE model took as input the powerpack rotor rpm. Which required a conversion from the vehicle speed to the rpm. Because the P519 engine has a fixed gear ratio this was easily done with formula 3.1 where N is the powerpack rpm and v is the car velocity in km/h. The tyre diameter D and gear ratio GR was provided to us by the Road Load and Customer Data team.

$$N = \frac{60 \cdot v \cdot \mathrm{GR}}{3.6 \cdot \pi \cdot D} \tag{3.1}$$

3.4 Iterative simulation process

As STAR-CCM+ 3D CFD model required the temperature of the E-machine, transmission and inverter housing surface temperatures as input those had to be supplied by the GT-SUITE 1D model that calculated the heat generated internally in the powerpack. But the extended GT-Suite model that calculates air cooling required both the air temperature of the engine bay air and the HTCs for the resistances between the thermal nodes that were in turn provided by the Star-ccm+ model for proper calibration. They were therefore dependent on values from each other to function properly which is why an iterative method had to be used for calibration.

Initially the internal variables for the operating condition was input into the original GT-Suite model that did not have the air cooling extension added. It was therefore only dependent on the internal variables of powerpack rpm (that is related to the vehicle speed because of the fixed gear ratio), engine torque and supplied voltage. This gave an initial estimate for the housing temperatures that were then used as input in the Star-ccm+ 3D model. In that model the remaining external variables of vehicle speed, radiator ejected heat, ambient temperature and fan speed were then additionally set and initialised. The stopping criteria was 10000 iterations

or once the heat ejection difference was below 1 Watt for 50 iterations in a row, whichever was lowest.

Once the 3D CFD simulation was complete the HTCs and temperatures were calculated. For surface temperatures, a surface average temperature function was used for the respective surfaces corresponding to the thermal nodes in GT-Suite. For the encapsulated air and the air in the engine bay the temperatures were calculated by averaging over a number of temperature probes which surrounded the powerpack as shown in fig 3.5. The heat transfer from or towards the powerpack was also measured. Lastly the HTCs were calculated with a custom function presented in equation 3.2 where $\dot{Q}$ was the heat flowing through the surface between the two thermal nodes, ΔT was the temperature difference and A was the area it travelled through.

$$HTC = \frac{\dot{Q}}{\Delta T \cdot A} \tag{3.2}$$

This function was used because the normal HTC function in Star-ccm+ uses a global reference temperature and it was in this case necessary to individually compare temperatures between nodes to fit with the GT-Suite model. It should be noted that the housing frames to inside encapsulation thermal node HTCs were calculated from the inside surface temperatures of the powerpack and not the outer surface temperatures of it. This was done to fit better with the thermal nodes in GT-Suite that more closely follow the inner temperature.

The calculated HTCs and the measured engine bay temperatures from full Car CFD simulations were then put into the full GT-Suite 1D model and the simulation was run. It should be noted that all HTC values used were the absolute value because the connections only accepts positive values. The heat transfer directions are governed by the temperature difference between the two thermal nodes on either side of the connections. The thermal node temperatures and heat transfers were compared with the 3D CFD measurements. If the bypass heat transfer results were within 1% (fulfilling inequality 3.3) of each other the model was considered to be converged and no further iterations were run. Otherwise the new housing temperatures from GT-Suite were put into the Star-ccm+ model and the previous steps repeated until convergence was achieved.

$$\left| \frac{\dot{Q}_{old} - \dot{Q}_{new}}{\dot{Q}_{old}} \right| \times 100 \leq 1.0 \tag{3.3}$$

3.5 Measurements

To gauge the capability and limitation of our 1D thermal model developed by us in this project we compared it with measurements data which is extracted from real driving conditions. The real driving test is done for 30 minutes with different vehicle speeds. As mentioned earlier our simulations are steady case. To have one to one comparison between the results, it is necessary to find the period of time in measurement data which has less variation in the value for over a period of time. This is the one limitation we have from the measurement data. By plotting the

required parameters with respect to time. Figure 3.6 shows the Temperature in deg °C for Transmission, E-Machine and Ambient air respectively. From figure 3.6, it is observed that Time period between 500 to 2000 sec shows more settled (Steady) values in the actual drive time. Hence, average temperature valued from measurement data is taken from between 500 to 2000 sec. Same trend is observed in Vehicle speed, Torque, coolant temperature shown in figure 3.7 & 3.8.

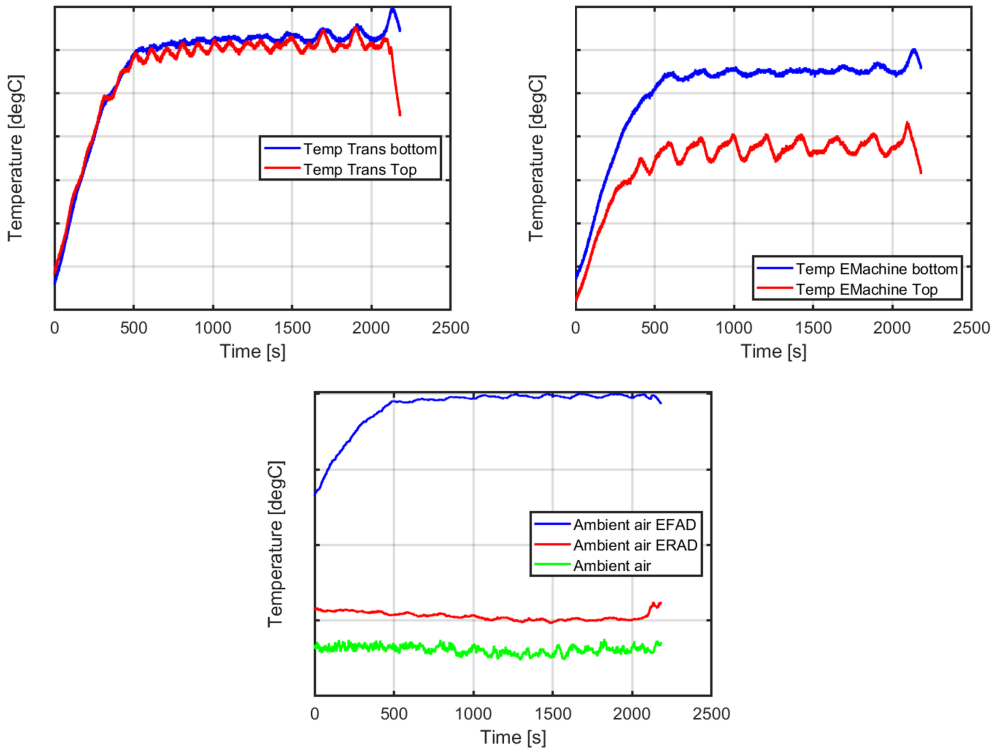

Figure 3.6: Plot of averaged temperature: Transmission, E-machine and ambient air

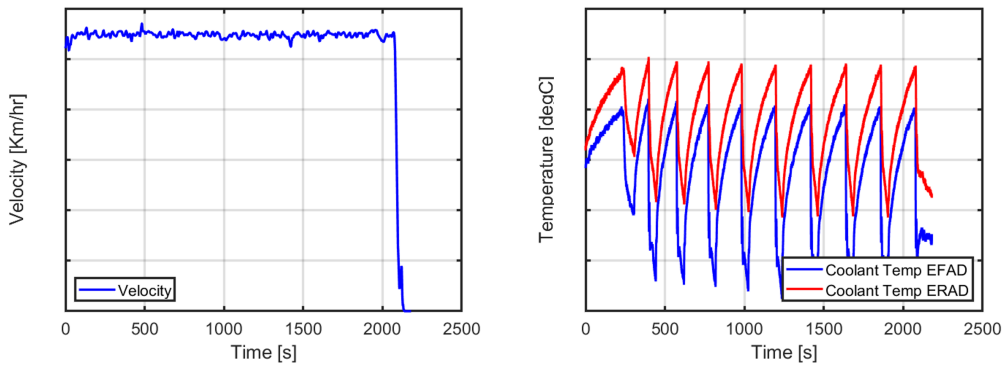

Figure 3.7: plot of Averaged velocity and Coolant temperature

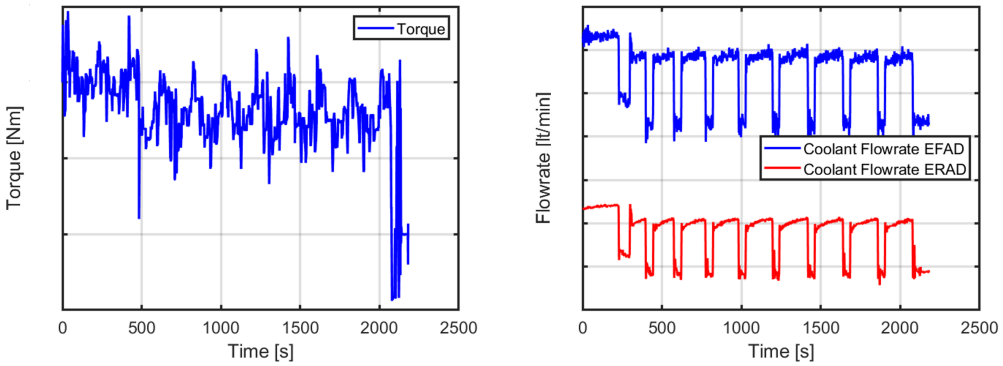

Figure 3.8: Plot of Averaged Torque and coolant flow-rate

4

Results

This chapter presents the results extracted from the finished GT-Suite model. First the effect of each variable on the temperatures and heat transfers are presented. After follows a few selected combined variable changes and a comparison between the new GT-Suite model with the air cooling extension with the old one without. Finally the new model is compared to physical measurements to verify its accuracy.

It was discovered during all the simulations that it always ran the maximum number of iterations but the results in Star-ccm+ plots seemed converged enough. The result later on in this chapter will show that 1 watt is a very small difference in comparison with the heat transfer explaining why the criteria was never used.

4.1 Variable Sweeps

As mentioned above this first section presents the effects of the input variables independently on the temperature and heat transfers. In the plots $Q_{air\ cooling}$ represents the combined heat flow through both the bypass connection and the encapsulation. Q_{total} is the total heat that is leaving the powerpack combined through the liquid- and air-cooling. Finally $Q_{internal\ losses}$ represents the total heat generated internally in the powerpack. As the model is a steady state model this should equal Q_{total} because no other paths for the heat to leave the powerpack exists in the model. This was shown to be true for all heat transfer figures shown below.

Only the EFAD results are shown here; the ERAD results look similar but with less variation in temperature and heat transfer over the variable sweeps. They also in general have less air cooling as a fraction of the total cooling. For ease of readability for the more significant EFAD results they have therefore been cut from this section and placed in the appendix.

4.1.1 Velocity

One of the variables that has the most effect on the cooling is the vehicle velocity. As it increases both the air cooling increases along with the total cooling as seen in figure 4.1. There is a peak in cooling at ∼70 km/h, especially for the liquid cooling. Afterwards the air cooling stays mostly constant up to 120 km/h while the liquid and therefore total cooling decreases. Finally they both increase for higher velocities.

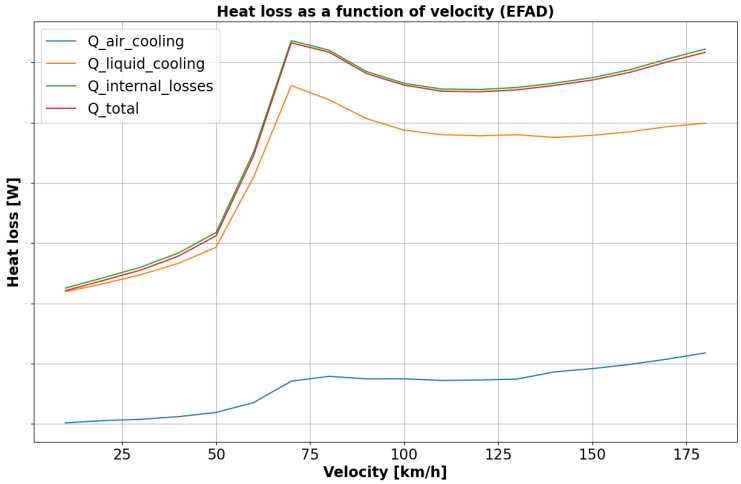

Figure 4.1: EFAD velocity sweep heat transfer

The air cooling increases faster with higher velocities than the liquid cooling does as figure 4.2 shows. At the highest velocity the air cooling is responsible for ∼20% of the total cooling and it is a significant component even at intermediate velocities. For all but the slowest velocities the direct bypass route represents the dominant part of the air cooling at above 90% of it.

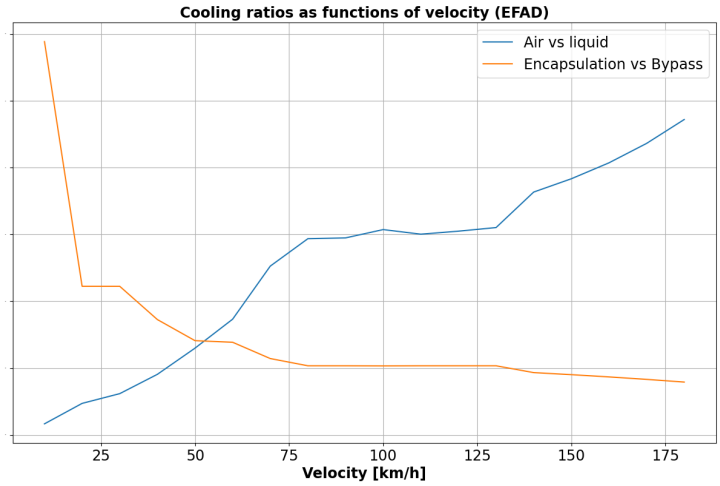

Figure 4.2: EFAD velocity sweep heat transfer ratios

Figure 4.3 shows the temperatures for a few selected surfaces. The highest ones are the E-machine and Transmission inner surfaces which makes sense because they are closest to the heat source and the heat must always flow from high temperature regions to colder ones. Both increases rapidly at lower velocities but at ∼70 km/h the E-machine temperature starts dropping substantially while the Transmission temperature only does so slightly and then returns to increase at higher velocities where the E-machine temperature stays mostly constant.

The temperature of the air close to the powerpack inside the encapsulation increases similarly at first but then declines as the velocity increases albeit very slowly. The encapsulation outer surface also decreases in temperature very slowly at higher velocities but stayed mostly constant at lower one. This shows the decreasing effect of the powerpack's impact when shielded from it by the encapsulation.

Finally the Engine Bay temperature only very slightly increases with higher velocities and even exhibits signs of decreasing at the higher ones. As the velocity is the only variable that is both external and internal to the powerpack this indicates that at higher velocities the cooling effect caused by the increased air convection outpaces the increased heat generated in the powerpack by the spinning driveshaft. This is also supported by the fact that the heat loss through air cooling stays constant and increases when the liquid heat loss decreases and stays constant at intermediate and higher velocities respectively.

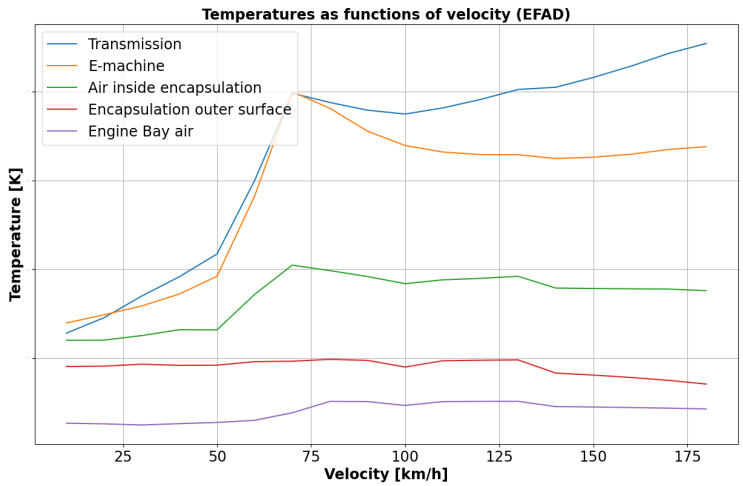

Figure 4.3: EFAD velocity sweep temperatures

4.1.2 Torque

Just as with the velocity sweep the heat losses increase with increasing torque as shown in figure 4.4. It increases over the whole range of torques without any peak. It does on the other hand increase slower after ∼150 Nm is reached. This figure does not show it clearly but at the very lowest value of torque the air cooling is actually negative. A negative heat transfer of -57.6 W of heat flowing from the engine bay air to the powerpack is found there.

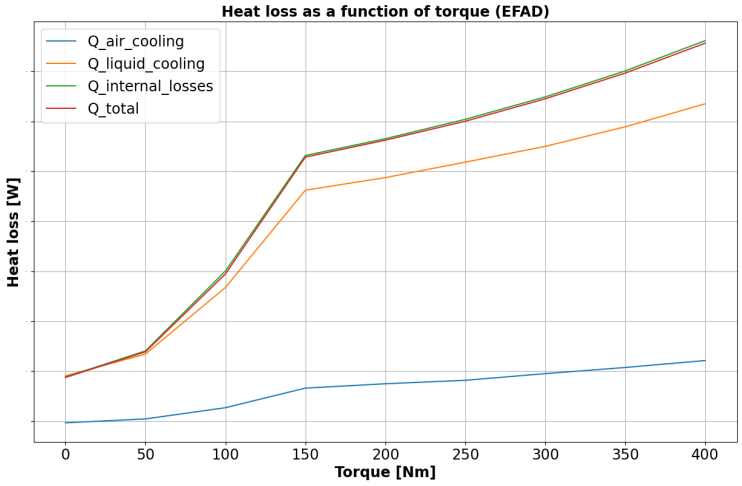

Figure 4.4: EFAD torque sweep heat transfer

Interestingly, figure 4.5 shows that the air cooling to liquid cooling ratio increases with increasing torque. The torque is a purely internal variable that should only increase the heat generated inside of the powerpack. The external HTCs outside of the powerpack should be unaffected by the torque value. The proportion of air cooling through the encapsulation is on the other hand stable at 5% except at really small torque values.

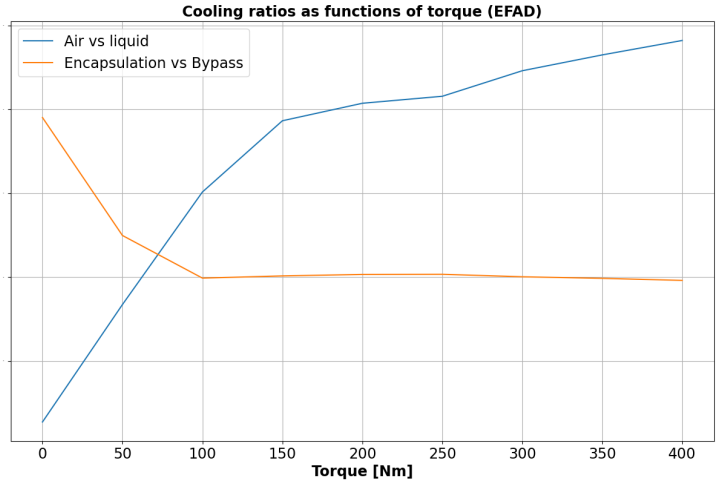

Figure 4.5: EFAD torque sweep heat transfer ratios

The temperatures of all the thermal nodes are in the correct order to maintain the heat flow from the powerpack to the engine bay air except at the lowest torque levels. Here the temperatures invert their order which fits well with the fact that the heat flow through air cooling is reversed as stated above. Figure 4.6 also shows that after the same torque value break-point as for the heat loss at ∼150 Nm the

temperature of the transmission starts to go up at a much faster pace than the E-machine temperature.

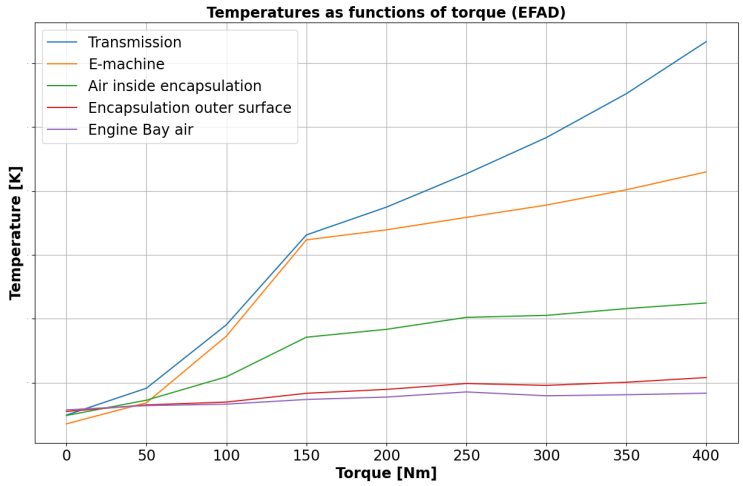

Figure 4.6: EFAD torque sweep temperatures

4.1.3 Voltage

Both the air and liquid cooling increases slightly up to 300 V and thereafter starts to decline quite rapidly as seen in figure 4.7. A higher voltage should lead to less current for the same power so the declining heat losses at the high voltages makes sense. The increasing ones for the lower voltages on the other hand are surprising.

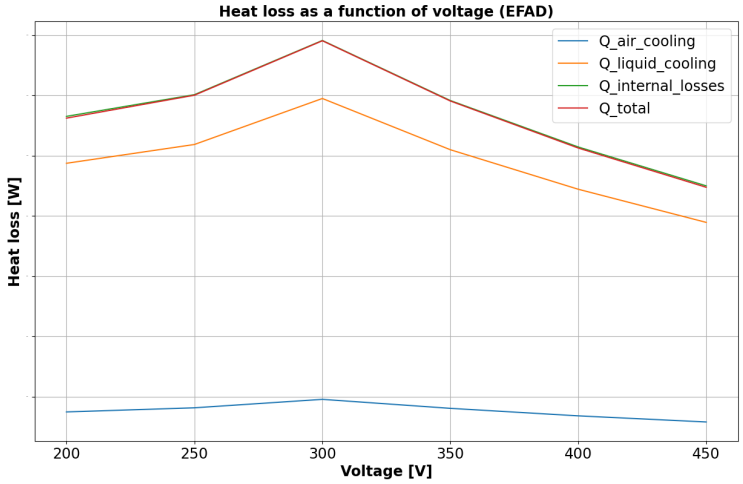

Figure 4.7: EFAD voltage sweep heat transfer

As the voltage is a purely internal variable only affecting the temperature of the powerpack it is as expected that the air to liquid cooling ratio shown in figure

4.8 is approximately constant for all voltage values. The ratio between bypass and encapsulation heat loss is also therefore constant.

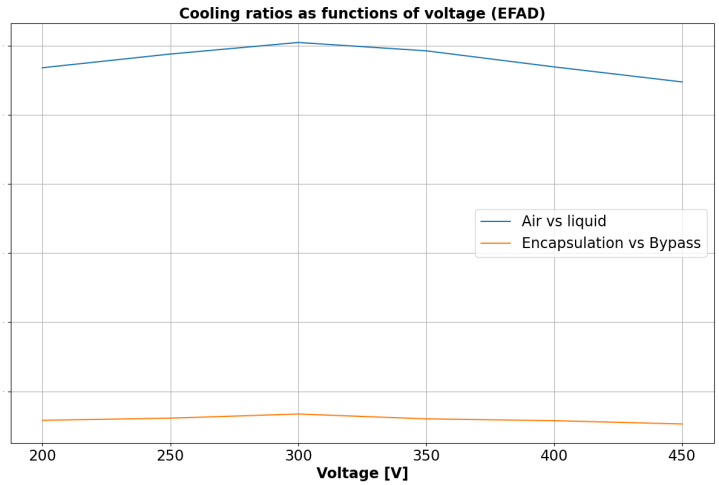

Figure 4.8: EFAD voltage sweep heat transfer ratios

The temperatures as a function of voltage as shown in figure 4.9 follows the heat loss in behaviour seen in figure 4.7. The transmission and E-machine temperatures follow each other over the entire voltage range with the transmission temperatures slightly higher. The air inside the encapsulation does the same at a lower value. The engine bay and encapsulation outer surface on the other hand only slightly change in temperature over the voltage range.

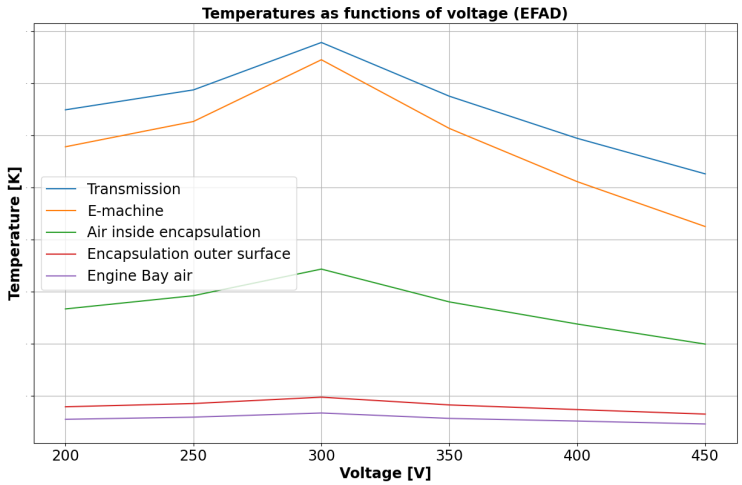

Figure 4.9: EFAD voltage sweep temperatures

4.1.4 Ambient Temperature

The ambient temperature outside of the car has little effect on the results except at the highest temperatures. Figure 4.10 shows that the heat transfer stays constant between the lowest ambient temperature at 260 K until around 290 K. There the air cooling starts to decrease slowly until it reaches the highest temperature measured at 308 K. It should be noted that while this is a decrease it only has a magnitude of about 150 watts so its importance is minor.

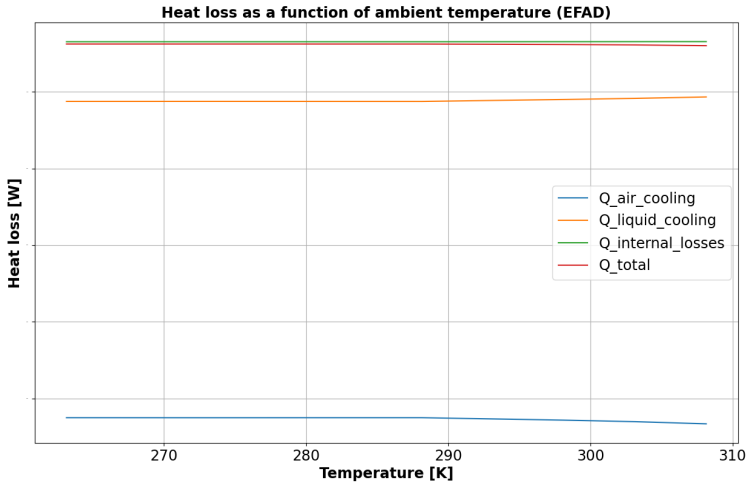

Figure 4.10: EFAD ambient temperature sweep heat transfer

Because the ambient temperature is external to the powerpack the same amount of heat is generated inside of it no matter the ambient temperature. Therefore when the air cooling drops off the liquid cooling compensates by slightly increasing. This fall in the air cooling fraction of the total is seen in figure 4.11. And as has been the case for all other cases so far the bypass route is responsible for ∼95% of the air cooling.

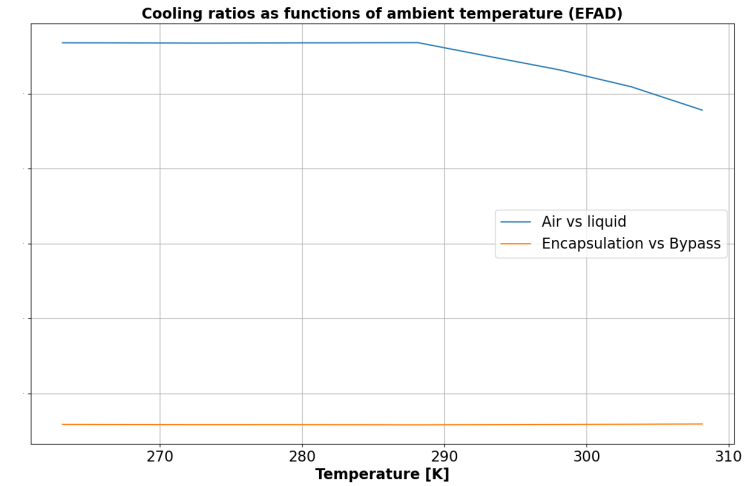

Figure 4.11: EFAD ambient temperature sweep heat transfer ratios

Figure 4.12 shows that the temperatures at all thermal nodes stays constant except at the highest temperatures. This is expected as when the temperature surrounding the powerpack increases the temperature of the surfaces also increases to maintain the total heat transfer. While the total heat transfer falls for most of the nodes, which means the temperature increase does not fully compensate for the ambient increase, the total cooling from the E-machine and Transmission frame stays the same. The temperature increase here does not only compensate to increase the air cooling but it also increases the liquid cooling temperature gradient and therefore the heat transfer.

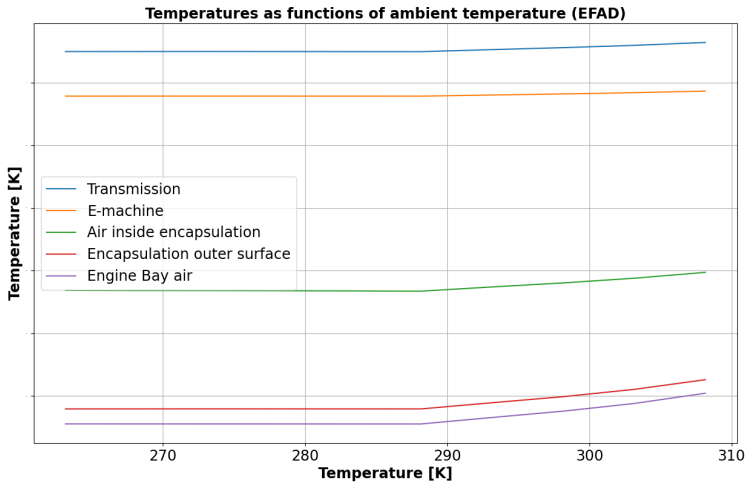

Figure 4.12: EFAD ambient temperature sweep temperatures

4.1.5 Radiator Ejected Heat

In contrast to the ambient temperature the heat the radiator ejects into the engine bay has a significant effect on the air cooling. Figure 4.13 shows that as it increases the heat transported through the air continually decreases over the whole simulated range. The liquid cooling likewise increases by the same amount to keep the total cooling constant as the internal powerpack heat generation is unaffected by the external variable.

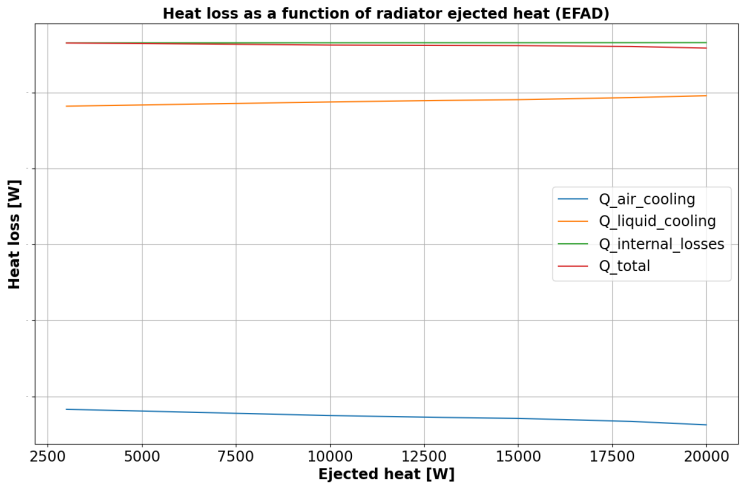

Figure 4.13: EFAD radiator ejected heat sweep heat transfer

As the total cooling stays mostly constant and the air cooling decreases it is expected that the air cooling ratio compared to the liquid cooling should decrease. Figure 4.14 shows that this is indeed the case. The proportion of the air cooling that passes through the encapsulation on the other hand stays mostly constant though a slight upward trend can be seen.

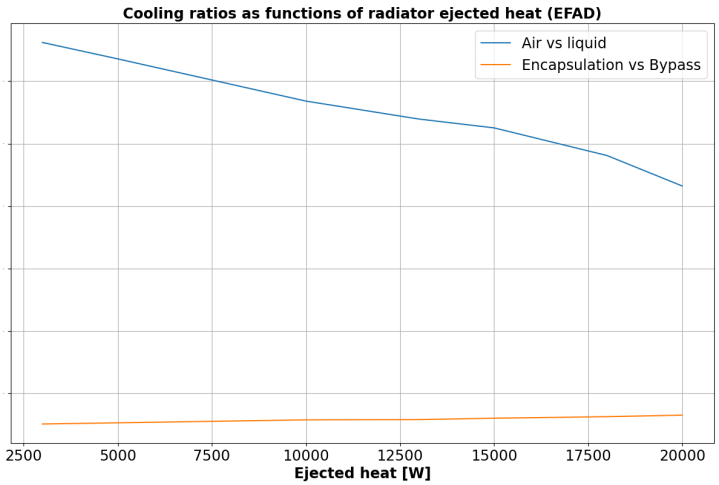

Figure 4.14: EFAD radiator ejected heat sweep heat transfer ratios

The temperatures shown in figure 4.15 shows that the engine bay, encapsulation outer surface and the air close to the powerpack temperatures increase significantly as the radiator dumps heat into the engine bay. The transmission and E-machine temperature also increases but less so as the liquid cooling is connected to them.

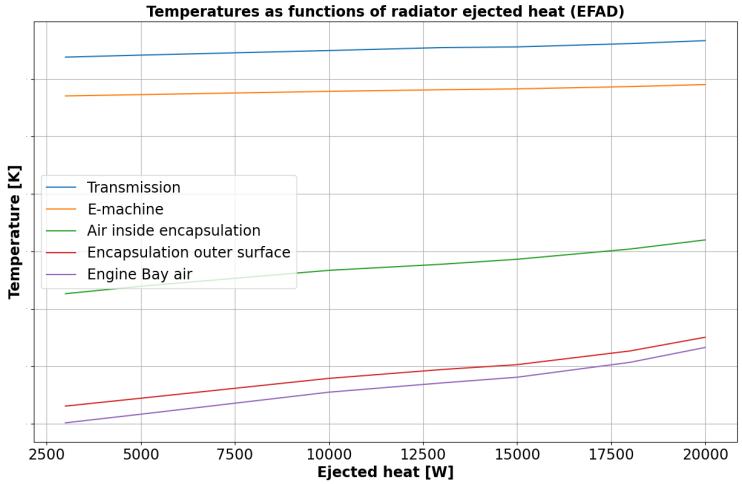

Figure 4.15: EFAD radiator ejected heat sweep temperatures

It should be noted that these relations were only seen in the EFAD results. The figures in appendix A.13, A.14 and A.15 shows no effect at all on the heat losses, ratios and temperatures with increasing radiator ejected heat. This makes sense because the radiator is located in the front part of the car and therefore only affects the temperature in the engine bay in the front part of the car.

4.1.6 Inlet Fan Speed

The fan in front of the car forcing air into the front engine bay does not seem to affect the cooling much as seen in figure 4.16 except the very highest fan speeds. There the air cooling increases slightly as the liquid cooling decreases. This indicates that the HTC values for the air cooling have increased which makes sense as a higher fan speed leads to a higher air speed velocity over the powerpack.

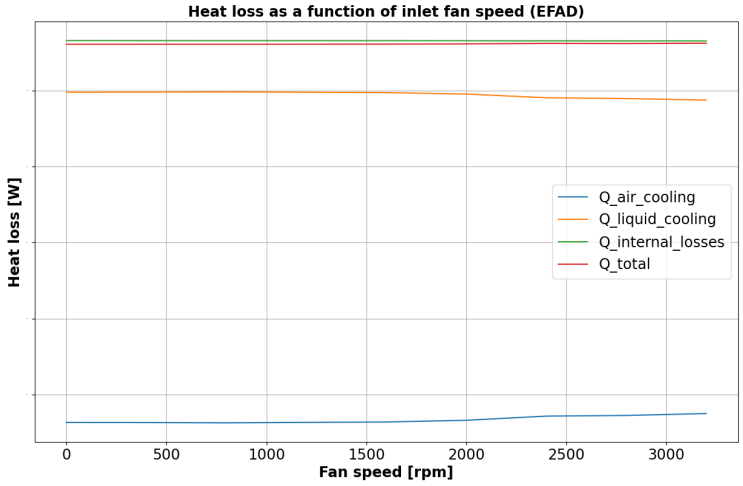

Figure 4.16: EFAD fan speed sweep heat transfer

This effect can also be seen in figure 4.17 as the air cooling vs liquid cooling ratio increases slightly at higher fan speeds and stays mostly constant at lower ones. Interestingly the fraction of air cooling through the encapsulation also slightly decreases at high fan speeds.

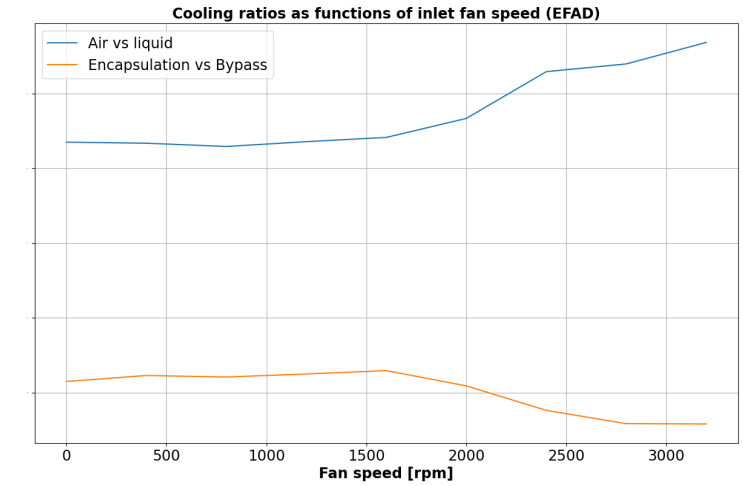

Figure 4.17: EFAD fan speed sweep heat transfer ratios

The temperature changes as a function of the fan speed are quite irregular as seen in figure 4.18. The transmission and E-machine temperatures follow what the heat loss plots show as they stay constant for low fan speeds and then decrease slightly in temperature where the air cooling increases. The other thermal nodes on the other hand do change with fan speed but has no clear relation to the heat loss or consistent relation to the fan speed.

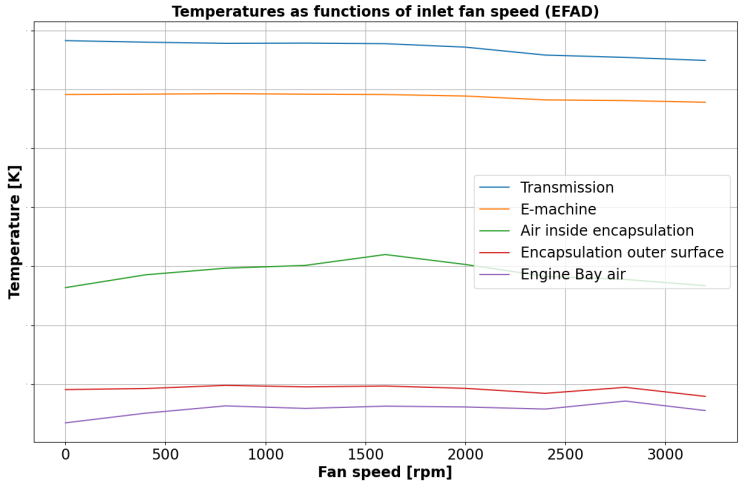

Figure 4.18: EFAD fan speed sweep temperatures

4.2 Combined variable changes from base case

In reality one variable rarely changes on its own so it is important to see how varying more than one variable at a time changes the results. As the velocity and torque sweeps gave the largest differences in heat transfer and temperatures these were chosen to be studied together. A total of 7 distinct cases were calculated; the first being the base case with 100 km/h car velocity and 200 Nm driveshaft torque. Then the four extreme points from the variable sweeps for the two variables at 10 and 180 km/h and 0 and 400 Nm respectively were calculated. Finally the two combined cases of these extreme points, that is one where the velocity is 10 km/h and the torque was 0 Nm and another where they were 180 km/h and 400 Nm were investigated. The results from those simulations can be seen in table 4.1 for the heat losses and in table 4.2 for the temperatures.

Table 4.1: Combined variable change for heat losses. For security reasons the actual values in watts have been normalised with the value of the total heat loss for the 100 km/h and 200 Nm case.

Velocity [km/h]	Torque [Nm]	$\dot{Q}$ Air [W]	$\dot{Q}$ Liquid [W]	$\dot{Q}$ Total [W]
100	200	0.122	0.878	1.00
10	200	0.003	0.396	0.398
100	0	-0.006	0.164	0.158
10	0	0.025	0.030	0.005
180	200	0.212	0.899	1.111
100	400	0.219	1.144	1.363
180	400	0.392	1.544	1.936

It can be seen that the effect of the two variables combine and amplifies each

other. Table 4.1 shows that when both the velocity and the torque increases all the heat losses increases more than for the equivalent single variable increases combined. The opposite can be seen when they both decrease. The combined case is still lower than for any one variable decrease alone but the effect is smaller than the one from both of them combined.

Table 4.2: Combined variable change temperatures

Velocity [km/h]	Torque [Nm]	T Bay [K]	T Encap Outer [K]	T Close [K]	T Emach [K]	T Trans [K]
100	200	315.5	317.9	336.7	367.8	374.9
10	200	317.6	318.0	324.0	327.9	325.6
100	0	311.5	311.0	309.8	307.1	309.9
10	0	315.6	314.1	302.3	295.5	297.7
180	200	311.0	314.1	335.1	367.6	390.8
100	400	316.7	321.6	345.0	386.0	426.7
180	400	314.5	321.5	365.1	411.7	511.3

The temperatures mostly follows the pattern the heat transfers indicate. When the air cooling heat flow is going out from the powerpack the surface temperatures decrease from the powerpack towards the engine bay. The exception is the 0 Nm torque and 100 km/h case where only the E-machine housing temperature is lower than the temperature of the air close to the powerpack. But the the transmission housing temperature is close enough to the "close" temperature that the heat transfer is minor and the total heat transfer can therefore still be flowing towards the powerpack.

Another interesting result is that for the 180 km/h and 400 Nm case the temperature is actually lower for the outer surface of the encapsulation and the engine bay than it is for the case where only the torque was increased from the base case. The other temperatures still increase though because the total heat generated in the powerpack has increased. This is most likely due to the increase in HTC value from the increased air velocity outside the encapsulation.

As the total power produced in the powerpack can be calculated with $P = \omega \cdot \tau$ where P is the power in watts, ω is the angular speed in radians per second and τ is the torque we can combine these two variables' internal effects and plot them as a function of produced power. The fixed relation between the vehicle speed and powerpack angular speed has already been described in formula 3.1 and combined with the 1 rad/s = $2\pi/60$ rpm conversion we get ω in the correct unit.

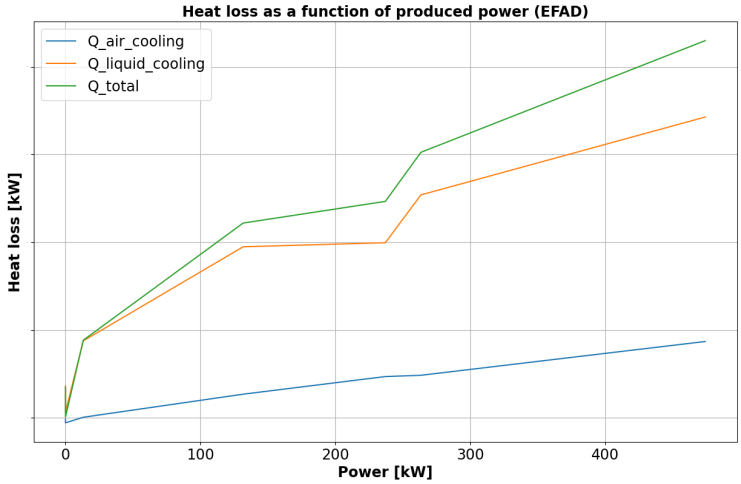

Figure 4.19: Heat loss as a function of power

The heat losses plotted as a function of these powers are displayed in figure 4.19. As expected, the general trend is that the heat losses increases with increasing power production but there are a few notable exceptions to this trend. There are two different values for the case of the produced power being zero and between 130 kW and 240 kW. The liquid cooling barely increases at all while the air-cooling does increase the same as before. Both of these are caused by the fact that the powerpack rpm has a fixed relation to the vehicle speed. Despite the torque being zero causing the power to also be zero the different vehicle speeds leads to different air cooling and therefore different results. Likewise, despite an increase in power the liquid cooling does not increase because as has been seen in figure 4.1 and 4.4 there exists a peak in generated heat in this region. The air cooling on the other hand still increases due to the higher vehicle speed giving a larger air cooling HTC.

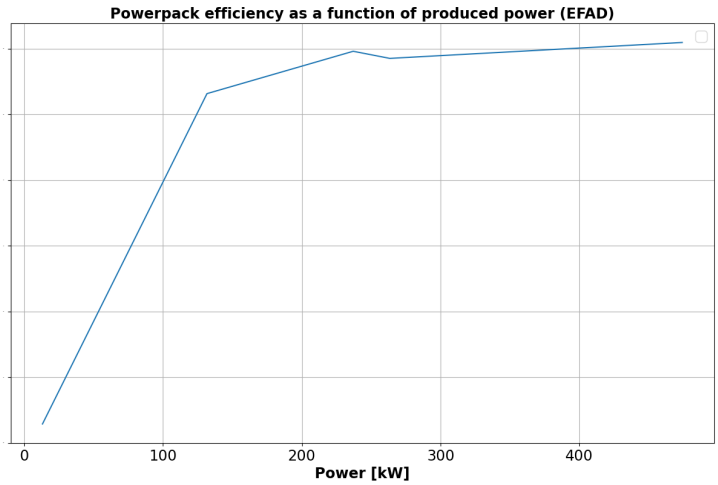

Figure 4.20: Powerpack efficiency

Figure 4.20 shows that the efficiency (that is the ratio of useful power in the driveshaft) increases with increasing total power production and eventually reaches equilibrium close to unity for intermediate and high power production. But as the power decreases the efficiency also decreases down to a minimum at around ∼60%.

4.3 Comparison with old model without air cooling

The older pre-existing model purely modelled all cooling through the cooling liquid while the newer model can do so through both the liquid and through the air. As such a comparison between the results from them can show the effect the air cooling has on the the heat loss and the temperatures. Only heat losses and temperatures that can be plotted in both models will be compared and the velocity variable sweep was chosen as it was seen to be one of the most impactful variables. ERAD results are placed in the appendix for readability of the EFAD plots and because the ERAD results generally show less difference between the models.

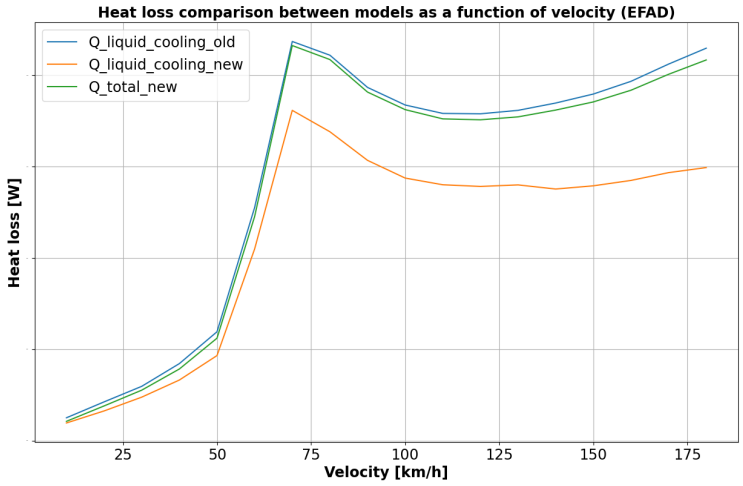

Figure 4.21: EFAD old vs new model comparison heat transfer

Figure 4.21 clearly shows that the heat loss through the liquid is significantly lower for the new model. This makes sense as there now exists an alternative cooling path through air that lessens the load on the liquid coolant. The total cooling from both the liquid and the air matches the old model's cooling through the liquid which it should because the heat generated in the powerpack should stay the same between the models. At lower velocities the air cooling contributes a minor part of the total cooling but at velocities higher than 70 km/h it starts having a larger effect. At those higher velocities the liquid cooling in the new model only needs to provide ∼80% of the cooling the old model predicts.

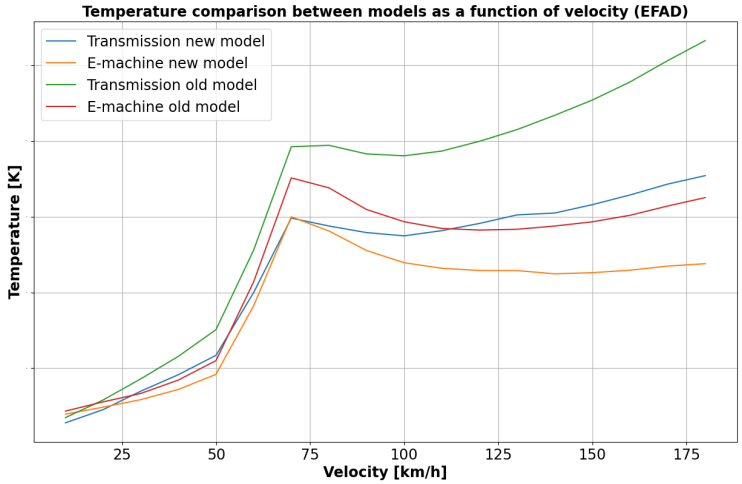

Figure 4.22: EFAD old vs new model comparison temperatures

The temperatures for the E-machine and the transmission are also different between the two models as seen in figure 4.22. As before the differences are not large before 70 km/h but afterwards the difference eventually reaches ∼20 K between the E-machine temperatures and ∼30 K between the transmission temperatures at the highest velocities. As the temperature is much lower than the old model predicted the amount of liquid cooling required to keep the surfaces under a certain temperature is now also much lower.

4.4 Verification of models with measurement data

To verify our model, Comparison is made between 1D simulations, 3D CFD simulations with the measurement data. As shown in figure (4.23 & 4.24) Probe is created in the same location in 3D CFD simulation as with temperature sensor used in measurements. The temperature value of 306.07K is found at that location in the 3D CFD simulation.

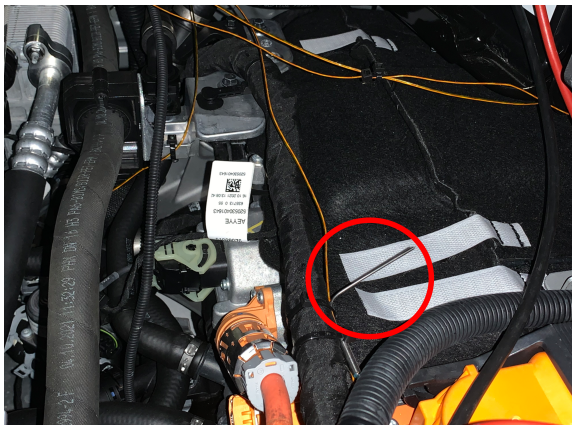

Figure 4.23: Probe position in actual test

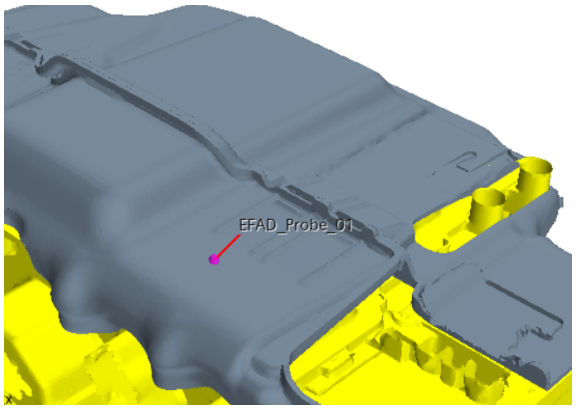

Figure 4.24: Probe position in 3D CFD simulation

Table 4.3: Temperature comparison with measurements

Temperature [K]	1D	3D	Measurements
E-Machine (outer)	N/A	315.18	312.39
Encap (Inner)	316.81	309.29	N/A
Encap (outer)	315.74	307.51	N/A
Inverter(outer)	N/A	303.19	N/A
Transmission (outer)	N/A	325.99	317.47
Avg probes Temp outside Encap	315.18	305.98	322.74
Avg probes Temp inside Encap	311.31	318.44	N/A

From the table 4.3, it is observed that temperature values are compared part-wise for EFAD between the models. To have one to one comparison, only temperature values outside the encapsulation is considered. Average temperature difference outside the Encapsulation is found be within +/- 10 deg which is acceptable. It is observed that both 1D and 3D simulation under predicts. In this case temperature values from 1D is more closer to measurements compared to 3D simulation. Between 1D and 3D model temperatures given by 3D under predicts the 1D by 6-8K.

The possible reason may be, the measurement data considered here is not a steady state. To compare the results from different methods, a single averaged value is taken over the actual drive cycle of 30 minutes. As mentioned in section 3.5, time period between 500 to 2000 sec is considered for averaging of temperature which exhibit somewhat steady state condition in the entire drive cycle. If comparison is made with exact steady state measurement data. Then, results between the models may match better.

Table 4.4: Heat transfer comparison between 1D and 3D for EFAD

sl no	Parts	Heat transfer in W for 3D	Heat transfer in W for 1D
1	Encap outer	-0.11	-0.06
2	Encap inner	-0.11	-0.06
3	E-machine (outer)	-0.95	-0.15
4	Inverter (outer)	0.07	0.37
5	Transmission (outer)	-1.78	-1.28
6	Bypass	-2.55	-1

Averaged values of measurement data (actual driving test) which is explained in Section 3.5 is not shown here due to confidentiality. In table 4.4, Heat transfer values are compared only between 1D and 3D simulation since they are not available from measurements. From the values tabulated in the above table, Heat transfer value don't show good match between 1D and 3D. In this case 1D simulation under predicts the Heat transfer values compared to 3D simulations.

5

Conclusion

This project aimed to accurately model the steady state heat transfer to and from the powerpack by air-cooling and relevant temperatures. As the 3D and 1D models were dependent on each other neither could verify the results by comparing with the other. What is known on the other hand is that for the simulated operating conditions they do match which proves that the GT-Suite model can accurately predict heat transfer and temperature values given the same input conditions.

When compared with physical measurements the 1D GT-SUITE model is not particularly accurate. While a difference in a few Kelvin otherwise would be good enough, in this case we have seen that it represents many hundred watts of difference in heat transfer. As the 1D and 3D models themselves do not agree with each other at the physical measurement operating condition, even though the combined variable change cases show the expected trend in heat transfer and temperature, we can conclude that the model in the current state is not ready. The exception to this being the variable sweeps it was calibrated on where by definition the 1D and 3D models agree with each other. To rectify this problem, calibration is needed on operating conditions representing all the possible combinations of the input variables.

What both the 3D and 1D models showed though was that the vast majority of the heat bypassed the NVH encapsulation. For all but the lowest values of velocity and torque $\sim$95% of the total air-cooling bypassed it. We can therefore conclude that the encapsulation is of minor importance for heat modelling purposes and most likely can be neglected in future projects. The temperature and HTC from the powerpack outer housing are the more important parameters to study.

Another interesting result was that the air cooling represented a substantial fraction of the total cooling. For high velocities it reached up to 20% of the total but not usually hovered around 15% during most variable sweeps. And as figure 4.22 shows, the temperatures of the powerpack frame was substantially lower when air cooling was modelled. We therefore see that it is important to model the air component of the cooling and that it cannot be neglected in favour of only modelling the liquid cooling.

Finally it was seen during the variable sweeps that they did not have equal effect on the results. The car velocity and driveshaft torque had by far the largest effect on the results. On the other hand the ambient temperature and the inlet fan speeds had minor effect on the heat transfer and the temperatures. It can therefore be concluded that at least when the other variables are set the same as the base case that these two variables are of little importance for the powerpack cooling.

5.1 Discussion and future work

It is not entirely clear that each variable behaves the same when varied no matter how the other variables are set up. Take the inlet fan speed for example. It had a minor effect during our simulations but the car was always travelling at 100 km/h during the entire variable sweep. As the fan essentially adds air speed over the powerpack it would not be out of the question that it would have a bigger effect at smaller car velocities. Similar effects that are dependent on other variables most likely exist for the other variables.

The idea of using a base case and varying each variable individually was done for time and computational limitations, it would have been preferable to also simulate every single combination of the chosen variable settings. The problem was that there were six variables so the amount of cases would be n^6 where n is the number of testing values for the variables which quickly becomes much too computationally expensive. If the number of variables could be reduced it might become more manageable.

There were also cases where the HTC sign did not match with the actual direction of the heat transfer. This limited what operating conditions we could run. All of these cases had in common that it was the probe determined "air inside the encapsulation" thermal node that had a connection where this mismatch happened. As the E-machine, transmission and inverter had significantly different surface temperatures the assumption that they all transferred heat into a common region that could be modelled with a single temperature is dubious. Therefore it would be better to model them separately if thermal nodes inside the encapsulation are still needed. But as most heat bypasses the encapsulation entirely they are most likely not needed. A model where the heat from the powerpack surfaces directly connects to the engine bay fixed temperature node would eliminate the problem inherent to averaging over distinctly different regions. It would also significantly simplify the GT-Suite 1D model.

Finally, the simulation criteria of a maximum of 1 watt difference for the last 50 run simulations was discovered to be too strict for the needed stability of the results. For future work it is recommended to relax the criteria to a wider range of watts.

Bibliography

[1] "CNBC". https://www.cnbc.com. https://www.cnbc.com/2021/04/29/global-electric-vehicle-numbers-set-to-hit-145-million-by-2030-iea-.html (accessed 2023-05-30).

[2] J. H. Lienhard IV and J. H. Lienhard, V, "The General Problem of Heat Exchange" in *A Heat Transfer Textbook*, 5th ed, Cambridge, Massachusetts, USA: Phlogiston Press, 2020, pp. 11-34, 63-69

[3] Siemens. "Simcenter STAR-CCM+". plm.automation.siemens.com. https://www.plm.automation.siemens.com/global/en/products/simcenter/STAR-CCM.html (accessed 2023-05-17).

[4] Gamma Technologies. "GT-SUITE, Integrated Multi-physics Systems Simulation". gtisoft.com. https://www.gtisoft.com/gt-suite/ (accessed 2023-05-17).

[5] J. Lindström, "Thermal Model of a Permanent-Magnet Motor for a Hybrid Electric Vehicle", Report No. 11R, ISSN: 1401-6176, Department of Electric Power Engineering, Chalmers University of Technology, Göteborg, Sweden, April 1999

A
Appendix

It was mentioned in the results section that the ERAD plots did not fit for readability reasons so they have been placed here. The reason the ERAD results specifically were removed from the main section was due to being less interesting. In general they show less air cooling both in absolute magnitude and as a fraction of the total cooling. The individual plots will therefore not be described in detail as they show the same results as the EFAD plots but with less air cooling.

A.1 ERAD variable sweep results

The the air cooling heat transfer was less effected by changes in the variables during the sweeps. It is believed that the reason for this is the obstruction of airflow caused by the powerpack's location at the back of the car. The inlet fan speed cannot effect the result because the fan only blows air on the front powerpack and the car speed velocity airflow which enters through the same inlet likewise cannot flow over the rear one. And as the car speed velocity was seen to be the most important variable for air cooling all other variable sweeps are dampened too.

A.1.1 Velocity

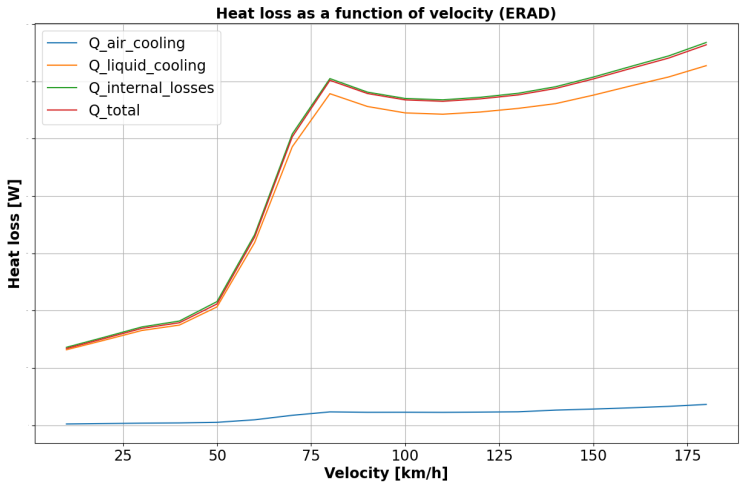

Figure A.1: ERAD velocity sweep heat transfer

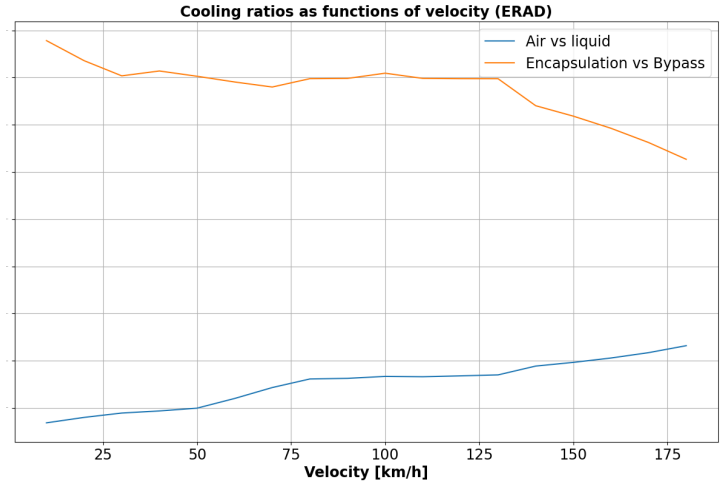

Figure A.2: ERAD velocity sweep heat transfer ratios

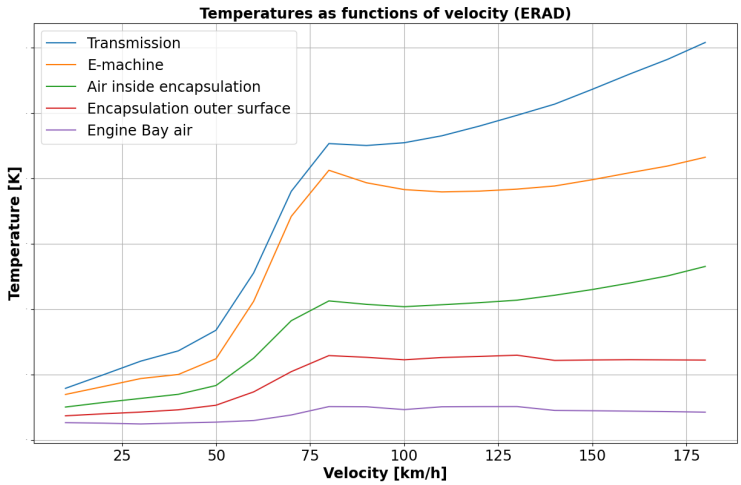

Figure A.3: ERAD velocity sweep temperatures

A.1.2 Torque

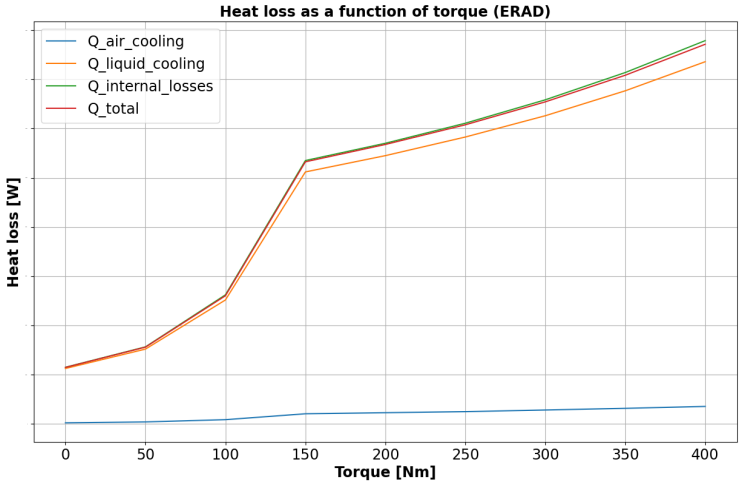

Figure A.4: ERAD torque sweep heat transfer

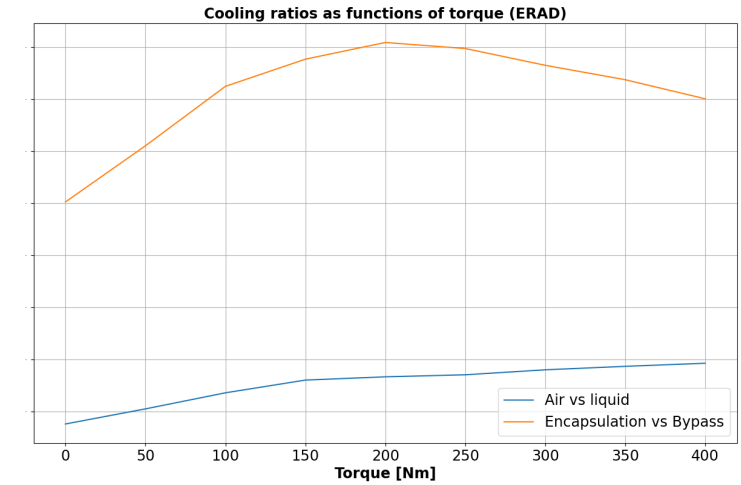

Figure A.5: ERAD torque sweep heat transfer ratios

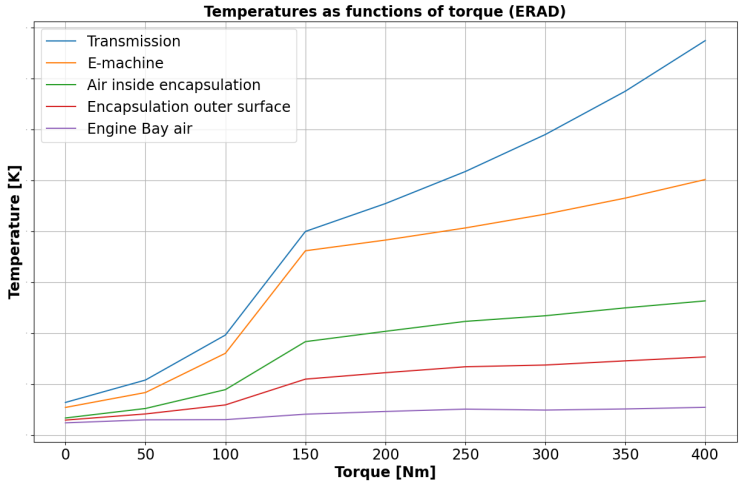

Figure A.6: ERAD torque sweep temperatures

A.1.3 Voltage

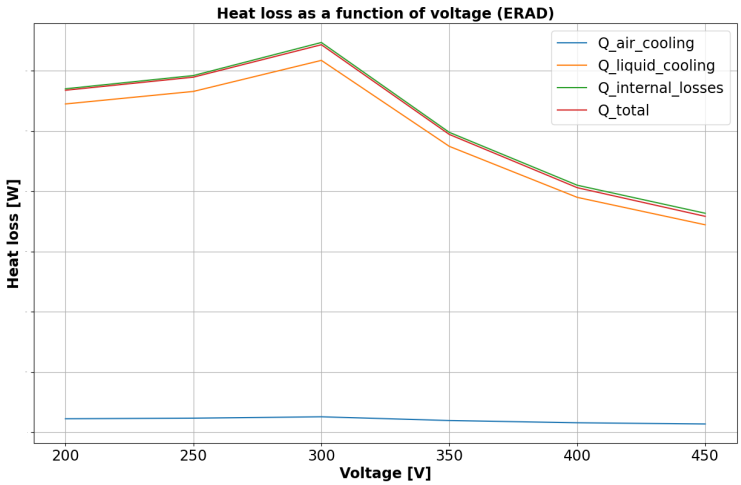

Figure A.7: ERAD voltage sweep heat transfer ratios

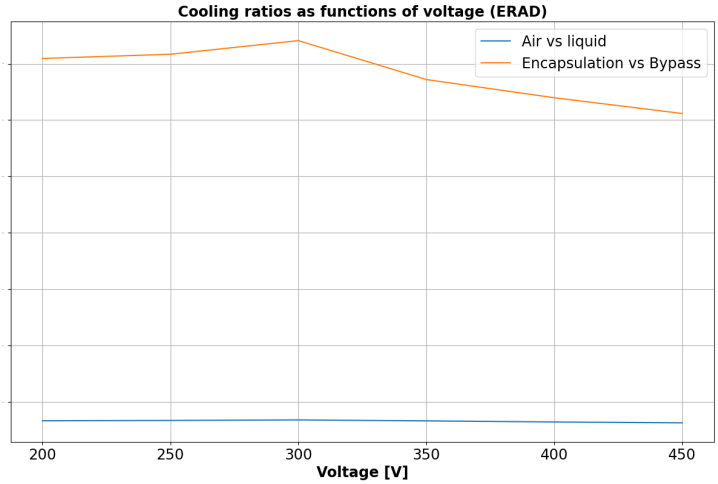

Figure A.8: ERAD voltage sweep heat transfer ratios

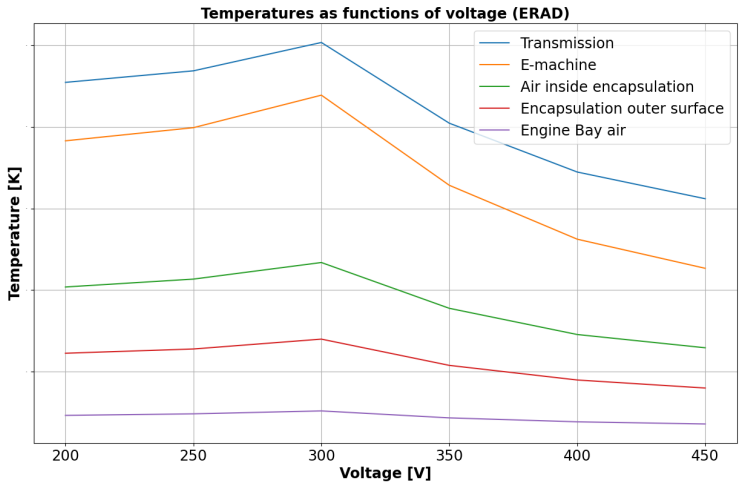

Figure A.9: ERAD voltage sweep temperatures

A.1.4 Ambient Temperature

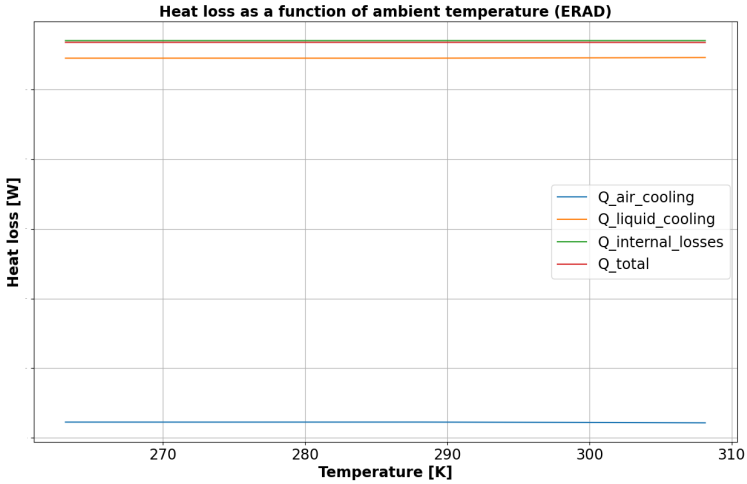

Figure A.10: ERAD ambient temperature sweep heat transfer

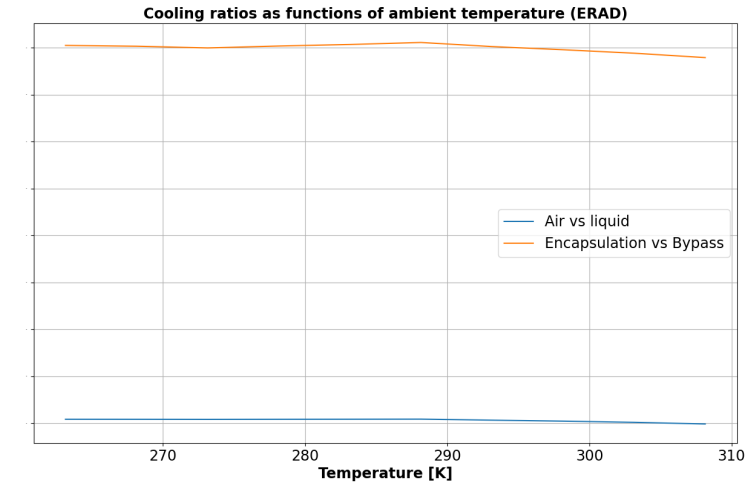

Figure A.11: ERAD ambient temperature sweep heat transfer ratios

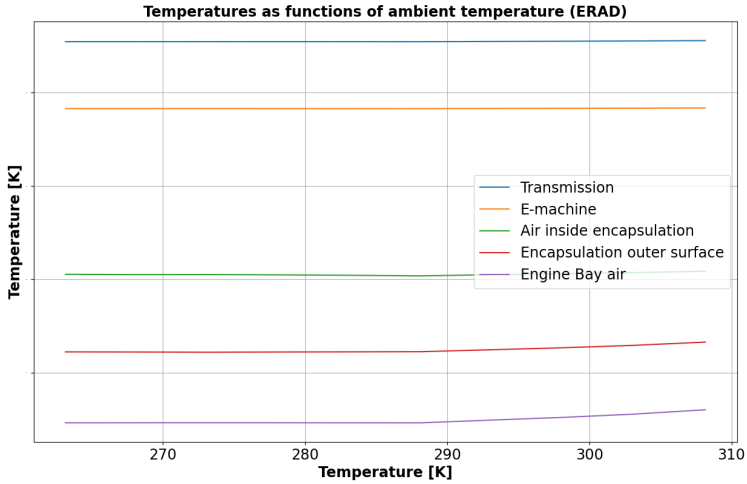

Figure A.12: ERAD ambient temperature sweep temperatures

A.1.5 Radiator Ejected Heat

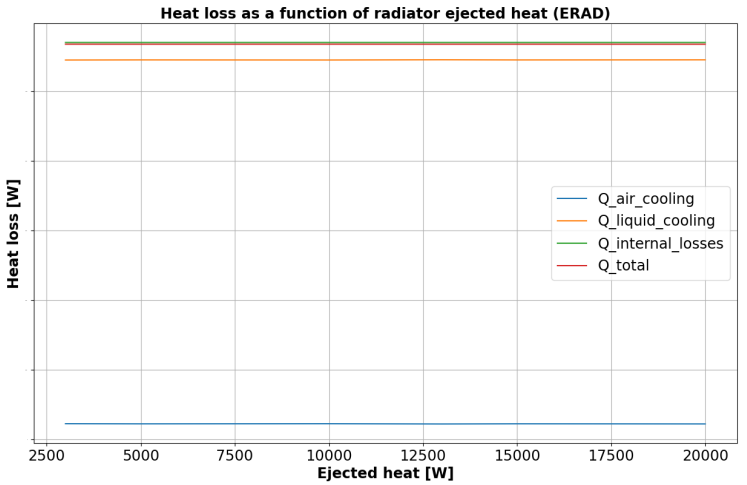

Figure A.13: ERAD radiator ejected heat sweep heat transfer

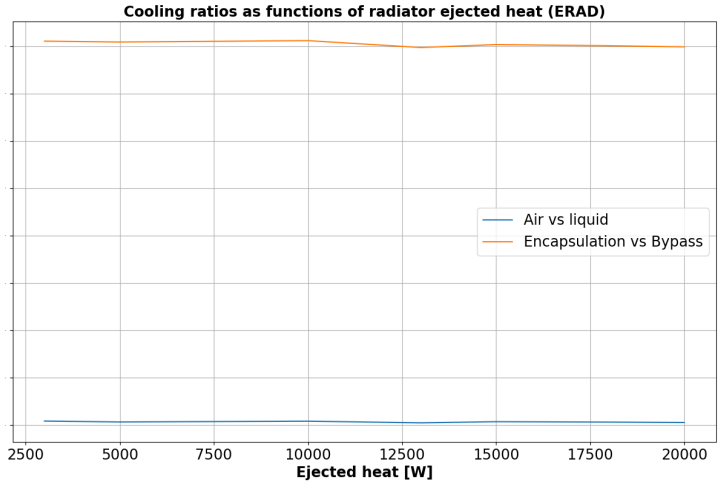

Figure A.14: ERAD radiator ejected heat sweep heat transfer ratios

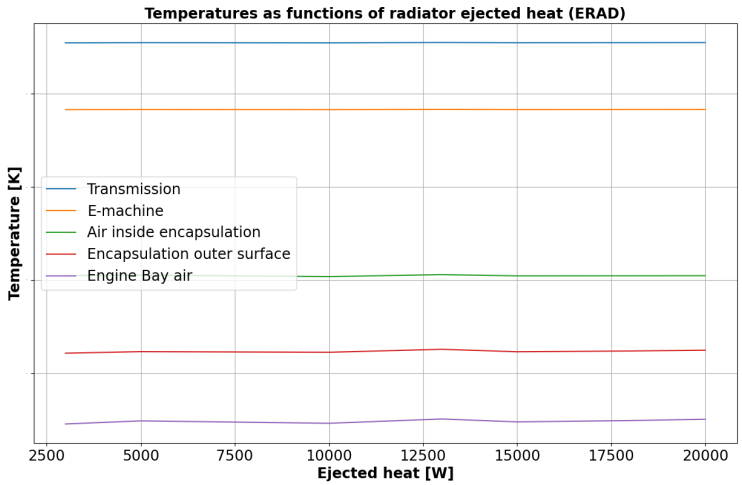

Figure A.15: ERAD radiator ejected heat sweep temperatures

A.1.6 Inlet Fan Speed

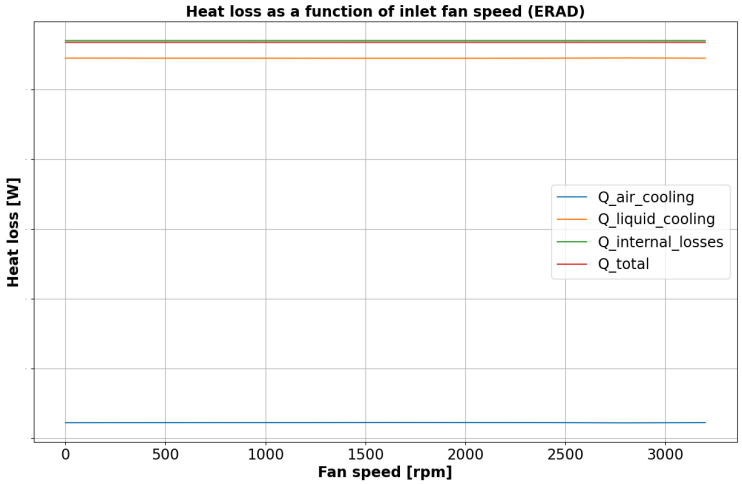

Figure A.16: ERAD fan speed sweep heat transfer

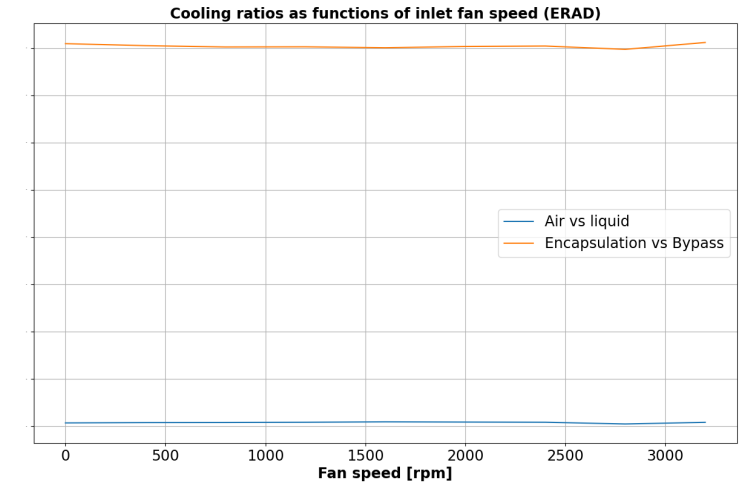

Figure A.17: ERAD fan speed sweep heat transfer ratios

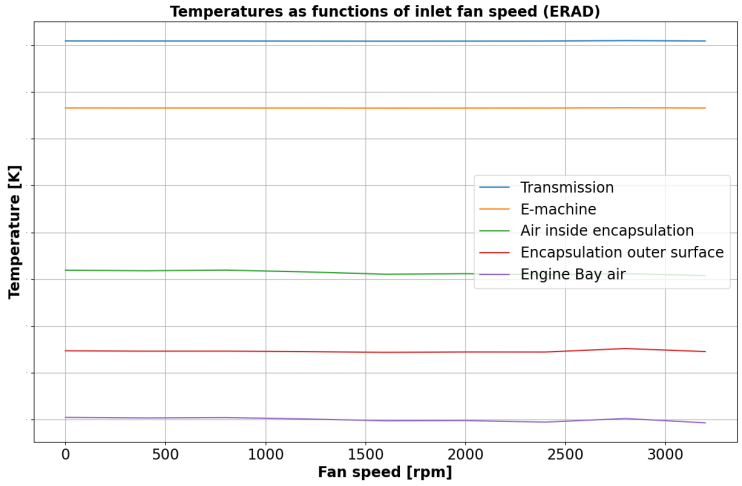

Figure A.18: ERAD fan speed sweep temperatures

A.2 ERAD comparison between old and new model

With less air cooling overall the difference between the old model without air cooling and the new one with air cooling becomes smaller. There still is a difference but it is much smaller than what is seen in figures 4.21 and 4.22 for the EFAD. Here in figure A.19 and A.20 both the heat loss and temperature curves follow each other closely with only a comparatively small gap in-between.

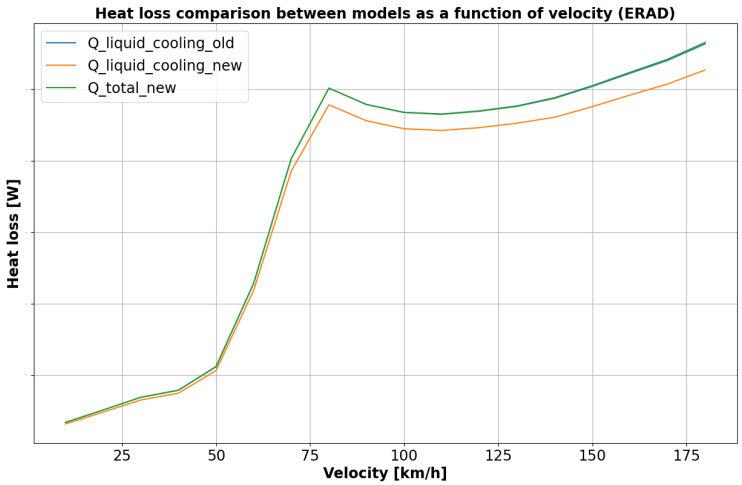

Figure A.19: ERAD old vs new model comparison heat transfer

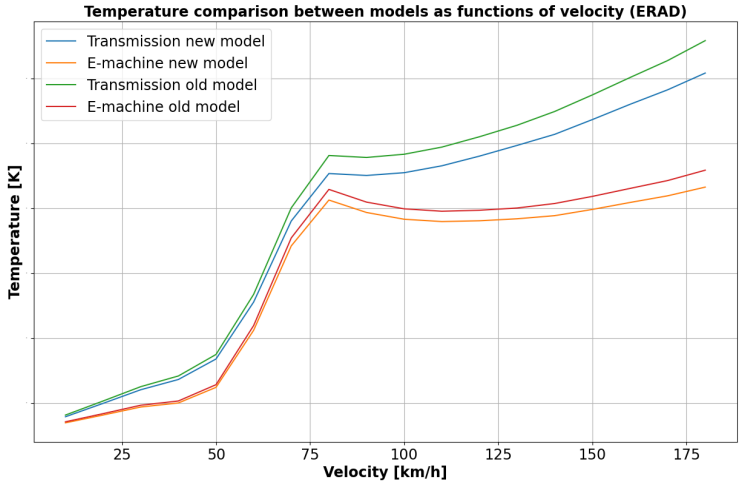

Figure A.20: ERAD old vs new model comparison temperatures

DEPARTMENT OF MECHANICS AND MARITIME SCIENCES
CHALMERS UNIVERSITY OF TECHNOLOGY
Gothenburg, Sweden
www.chalmers.se

CHALMERS
UNIVERSITY OF TECHNOLOGY